

## PUBLISHER :



Address of Publisher  
& Editor's Office :

GDAŃSK UNIVERSITY  
OF TECHNOLOGY

Faculty  
of Ocean Engineering  
& Ship Technology

ul. Narutowicza 11/12  
80-952 Gdańsk, POLAND  
tel.: +48 58 347 17 93  
fax : +48 58 341 47 12  
e-mail : sekoce@pg.gda.pl

Account number :  
**BANK ZACHODNI WBK S.A.**

I Oddział w Gdańsku  
41 1090 1098 0000 0000 0901 5569

### Editorial Staff :

**Witold Kirkor** Editor in Chief  
e-mail : pmrs@op.pl

**Maciej Pawłowski** Editor for review matters  
e-mail : mpawlow@pg.gda.pl

**Tadeusz Borzęcki** Editor for international relations  
e-mail : tadbtor@pg.gda.pl

**Cezary Spigarski** Computer Design  
e-mail : biuro@oficynamorska.pl

Domestic price :  
single issue : 20 zł

Prices for abroad :  
single issue :  
- in Europe EURO 15  
- overseas US\$ 20

ISSN 1233-2585

Special Issue 2006/S1  
published by:  
[www.oficynamorska.pl](http://www.oficynamorska.pl)



# POLISH MARITIME RESEARCH

*in internet*

[www.bg.pg.gda.pl/pmr.html](http://www.bg.pg.gda.pl/pmr.html)



## POLISH MARITIME RESEARCH

Special Issue 2006/S1

### CONTENTS

- 5 **BOSHIDAR METSCHKOW**  
*Sandwich panels in shipbuilding*
- 9 **JANUSZ KOZAK**  
*Problems of strength modelling of steel sandwich panels under in-plane load*
- 13 **JANUSZ KOZAK**  
*Fatigue life of steel laser-welded panels*
- 17 **RYSZARD PYSZKO**  
*Strength assessment of a version of joint of sandwich panels*
- 21 **MARIAN BOGDANIUK, ZENON GÓRECKI, MARIUSZ BRZÓSKA**  
*FEM analysis of ultimate strength of steel panels*
- 24 **MAREK AUGUSTYNIAK, GRZEGORZ POREMBSKI**  
*FEM strength analysis of sandwich panels for ship structure applications*
- 27 **DARIUSZ BOROŃSKI, JÓZEF SZALA**  
*Fatigue life tests of steel laser-welded sandwich structures*
- 31 **DARIUSZ BOROŃSKI, JÓZEF SZALA**  
*Tests of local strains in steel laser-welded sandwich structure*

The papers published in this issue have been reviewed by :

*Assoc. Prof. T. Kucharski*

*Prof. K. Rosochowicz*

# Editorial

---

POLISH MARITIME RESEARCH is a scientific journal of worldwide circulation. The journal appears as a quarterly four times a year. The first issue of it was published in September 1994. Its main aim is to present original, innovative scientific ideas and Research & Development achievements in the field of :

## **Engineering, Computing & Technology, Mechanical Engineering,**

which could find applications in the broad domain of maritime economy. Hence there are published papers which concern methods of the designing, manufacturing and operating processes of such technical objects and devices as : ships, port equipment, ocean engineering units, underwater vehicles and equipment as well as harbour facilities, with accounting for marine environment protection.

The Editors of POLISH MARITIME RESEARCH make also efforts to present problems dealing with education of engineers and scientific and teaching personnel. As a rule, the basic papers are supplemented by information on conferences , important scientific events as well as cooperation in carrying out international scientific research projects.

## Scientific Board

---

Chairman : Prof. **JERZY GIRTLER** - Gdańsk University of Technology, Poland

Vice-chairman : Prof. **ANTONI JANKOWSKI** - Institute of Aeronautics, Poland

Vice-chairman : Prof. **MIROSLAW L. WYSZYŃSKI** - University of Birmingham, United Kingdom

---

Dr **POUL ANDERSEN**  
Technical University  
of Denmark  
Denmark

Prof. **STANISŁAW GUCMA**  
Maritime University of Szczecin  
Poland

Prof. **YASUHIKO OHTA**  
Nagoya Institute of Technology  
Japan

Dr **MEHMET ATLAR**  
University of Newcastle  
United Kingdom

Prof. **ANTONI ISKRA**  
Poznań University  
of Technology  
Poland

Prof. **ANTONI K. OPPENHEIM**  
University of California  
Berkeley, CA  
USA

Prof. **GÖRAN BARK**  
Chalmers University  
of Technology  
Sweden

Prof. **JAN KICIŃSKI**  
Institute of Fluid-Flow Machinery  
of PASci  
Poland

Prof. **KRZYSZTOF ROSOCHOWICZ**  
Gdańsk University  
of Technology  
Poland

Prof. **SERGEY BARSUKOV**  
Army Institute of Odessa  
Ukraine

Prof. **ZYGMUNT KITOWSKI**  
Naval University  
Poland

Dr **YOSHIO SATO**  
National Traffic Safety  
and Environment Laboratory  
Japan

Prof. **MUSTAFA BAYHAN**  
Süleyman Demirel University  
Turkey

Prof. **JAN KULCZYK**  
Wrocław University of Technology  
Poland

Prof. **KLAUS SCHIER**  
University of Applied Sciences  
Germany

Prof. **MAREK DZIDA**  
Gdańsk University  
of Technology  
Poland

Prof. **NICOS LADOMMATOS**  
University College London  
United Kingdom

Prof. **FREDERICK STERN**  
University of Iowa,  
IA, USA

Prof. **ODD M. FALTINSEN**  
Norwegian University  
of Science and Technology  
Norway

Prof. **JÓZEF LISOWSKI**  
Gdynia Maritime University  
Poland

Prof. **JÓZEF SZALA**  
Bydgoszcz University  
of Technology and Agriculture  
Poland

Prof. **PATRICK V. FARRELL**  
University of Wisconsin  
Madison, WI  
USA

Prof. **JERZY MATUSIAK**  
Helsinki University  
of Technology  
Finland

Prof. **TADEUSZ SZELANGIEWICZ**  
Technical University  
of Szczecin  
Poland

Prof. **WOLFGANG FRICKE**  
Technical University  
Hamburg-Harburg  
Germany

Prof. **EUGEN NEGRUS**  
University of Bucharest  
Romania

Prof. **WITALIJ SZCZAGIN**  
State Technical University  
of Kaliningrad  
Russia

Prof. **BORIS TIKHOMIROV**  
State Marine University  
of St. Petersburg  
Russia

Prof. **DRACOS VASSALOS**  
University of Glasgow  
and Strathclyde  
United Kingdom

## Coordinator's message



*This is a special issue of the Polish Maritime Research quarterly, focused on aspects of basic properties and problems of application of new structural elements for ship hull structures, i.e. laser-welded steel sandwich panels. In order to apply such new idea instead of the "classical" design consisting in shell plating supported by a system of heavy stiffeners perpendicular to it, it is necessary to know its strength, corrosion, vibration, fire resistance and fatigue characteristics, to demonstrate to classification societies that its properties are not worse than those of classical structure. This was the aim of the EU-supported EUREKA project ASPIS hence the presented papers are based upon results of the research carried out within the frame of the project..*

**Project Coordinator: Janusz Kozak, D.Sc., Eng.**

# **ALL STEEL SANDWICH PANELS – – AN ALTERNATIVE FOR CLASSICAL SHIP HULL STRUCTURE**

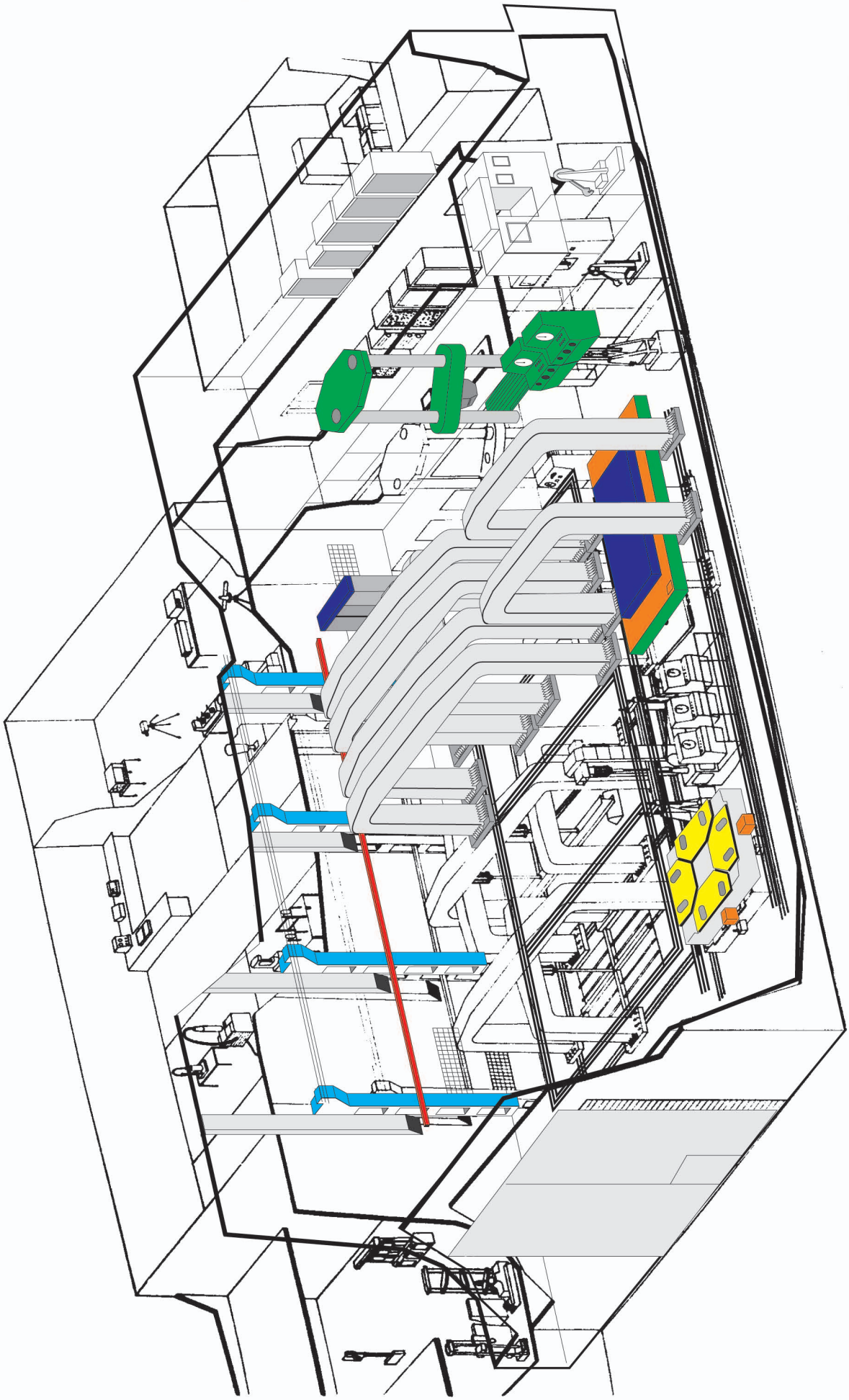
**Project Eureka E!3074**  
*Application of Steel Sandwich Panels  
Into Ship Structural Design*  
**ASPIS**

**Chief executor and coordinator  
of the project :**

***Gdańsk University of Technology  
Faculty of Ocean Engineering  
and Ship Technology***

**Gdańsk 2006**





# Sandwich panels in shipbuilding

**Boshidar Metschkow**, Assoc. Prof.  
Gdańsk University of Technology

## ABSTRACT



*In this paper a short historical outline of laser technique development and its application to welding sandwich panels, is presented. Laser-welded sandwich panels of different geometry, today introduced in industrial scale, were described. Prefabrication process of folded ship constructions, in particular, of panel-to-panel connections and hybrid (sandwich panel – conventional construction) structures, was discussed. Attention was paid to various aspects of prefabrication, assembly and use of panel constructions.*

**Keywords** : laser welding, laser - welded steel panels, I-core panels, connection of panels, double skin structure, ship structures

## INTRODUCTION

Industrial use of the laser radiation started in the 1960s. The ideas of Einstein, theoretically explained in the years 1914-1919, were developed in 1950 in the USA by A.L. Schawlow and C. H. Townes who provided fundamentals of the process. Continuation of the work, carried out also by Basow and Prochorow during the years 1953-1954, showed that forced emission of energy by microwaves is possible in the laboratory-scale. As a result the first MASER (Microwave Amplification by Stimulated Emission of Radiation) was built by Townes and his collaborators, Gordon and Zeiger, in 1954.

Some years later, in 1960, an optical maser was built in the laboratory of the Hughes Aircraft Company, California. Under the name LASER (Light Amplification by Stimulated Emission of Radiation) it has brought revolutionary changes into many fields of technique, medicine, optics, astronomy etc.

The main advantage of the laser beam comes from its enormous density of energy as compared with conventional sources of energy. The laser beam energy density ranges from  $10^8$  to  $10^9$  W/cm<sup>2</sup> whereas conventional welding procedures, such as the hand electrode welding, offers only  $10^4$  W/cm<sup>2</sup>, and TIG (tungsten inert gas) process -  $10^5$  W/cm<sup>2</sup>. This is still higher even than that of other new welding processes with high-energy output – such as the plasma welding process -  $10^6$  W/cm<sup>2</sup> or the electron beam welding -  $10^7$  W/cm<sup>2</sup>. Such high energy density leads to an essential increase of speed of welding process, a perceptible reduction of the deformation energy, and consequently, to minimization of the unwanted post-welding deformations. It was the base to start – in 1990 – intensive work aimed at the introduction of laser welding technique into the shipbuilding industry.

## LASER-WELDED PANELS – AN INNOVATIVE STRUCTURAL SOLUTION

The development of laser technique brought to building CO<sub>2</sub> lasers of about 20 kW power and ruby ones of 6 kW power, opened the way to the application of laser welding in shipbuilding. The introduction of such technique required, however, the creation of laser-weldable ship structures – as the first step. Because of the higher demands concerning joint preparation it was not possible to simply take over the ship hull “classical” construction consisting of plating and crossing stiffeners. Fig.1 presents a comparison of the classical (conventional) ship structure – for which the advantages of the laser welding could not be exploited

in the initial development stage – with the sandwich panel structure prepared to the laser hybrid welding process (laser welding combined with MAG – metal active gas welding).

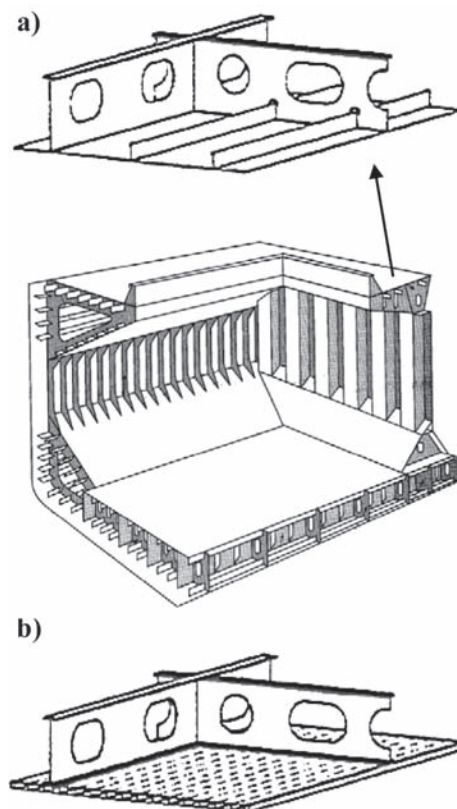


Fig. 1. Ship structure: a) classical (conventional), b) sandwich [1].

Since industrial lasers are currently built as stationary installations (Fig.2), the research is focused on production of the stiffened flat (or weakly bent) plate sections (Fig.1a and 1b). A conventionally stiffened flat section has an orthogonal stiffening system consisted of the rolled bulb or angle profiles in one direction, and welded T-beams in the second one. Large length of the fillet welds to be welded, combined with the introduction of considerable amount of heat constitute the factors reducing productivity and production quality. A hybrid structure (created from a laser-welded panel and one-directional T-beam) can be used instead, so the numerous stiffeners of the first direction can be omitted hence to reduce all the above-mentioned problems (Fig 1b).





Fig. 2. Laser welding machine for panels of up to 12 m in length [2].

The mentioned laser-welded panel consists of two shell plates between which is mounted one-directional stiffener system. The stiffeners are connected with the plates by laser welding executed from outside of the plates. Principle of the process is shown in Fig.3. The laser beam penetrates the shell plate through and the end of the adjacent stiffener and joins this way both the elements.

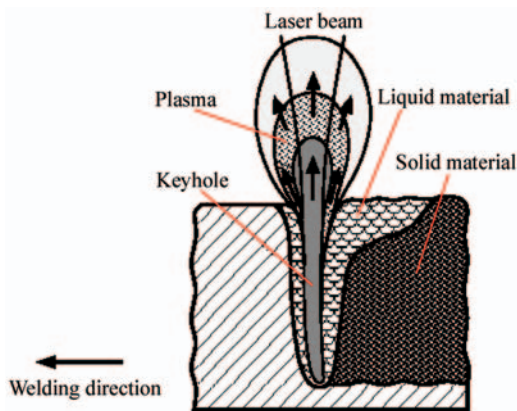


Fig. 3. Depth effect of the laser beam [3].

Panels welded in such manner show smaller welding deformations and have a better flatness in comparison with conventional structures. The laser-welded panel is shown in Fig.4.

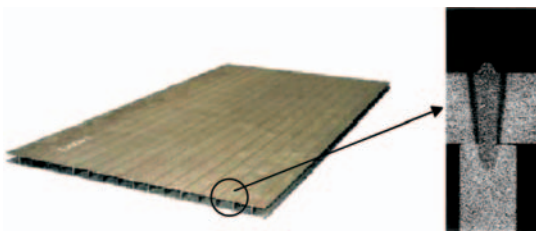


Fig. 4. Laser-welded panel fitted with flat steel stiffeners (webs) – (I-core) [4].

The industrially produced I-core panels can be made in a variety of geometrical dimensions as follows: shell plating thickness from 1.5 to 10 mm, panel width from 500 to 3 000 mm, panel length from 1 000 to 10 000 mm, panel depth from of 40 to 100 mm, stiffener spacing from 80 to 120 mm, minimum stiffener thickness of 3 mm. The joining method in question offers possible application of different geometries of internal stiffeners, for example: X-core, V-core, L-core, O-core, Z-core and other (see Fig.5).

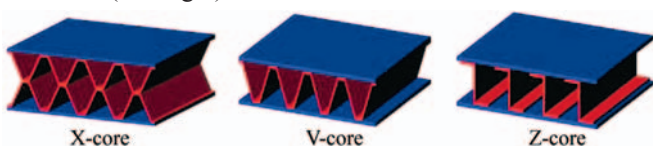


Fig. 5. Different forms of core of sandwich panels [5].

From the shipbuilding point of view, I-core panels seem to be the most suitable because they have an optimal relation of its mass to stiffness both in the longitudinal and transverse direction, and are relatively easy for manufacturing.

Beside of these completely flat, also panels with one-directional curvature can be manufactured. Such panels can be used for example for roofing huge halls or covering concrete walls. An example of the panel with one-directional curvature is presented in Fig.6.

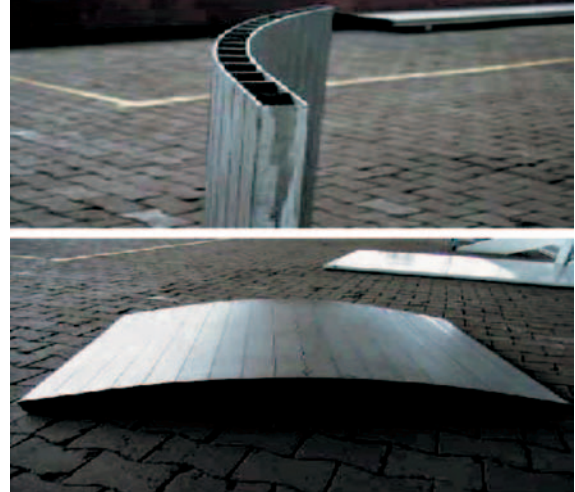


Fig. 6. Laser-welded panel with one-directional curvature [6].

For the improvement of the stiffness or for raising other properties such as sound insulation, the panel's interior can be filled with an additional material such as expanded polyurethane, balsa wood or lightweight concrete. Such core material can also improve corrosion resistance or reduce thermal conductivity. The application of the core material also improves buckling strength of the shell plates.

The shell plate buckling between supporting stiffeners is one of the most important problems in the dimensioning of steel sandwich structures. The small thickness of shell plating leads to a relatively small value of critical buckling stresses. The critical load can be increased by the supporting effect of the filling. As an example, the panel with lightweight concrete filling is presented in Fig.7.

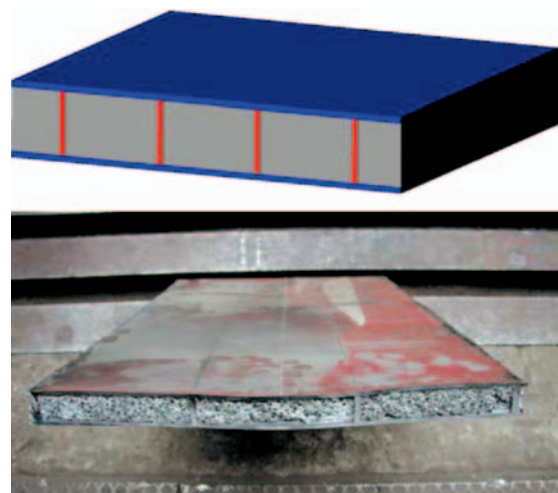


Fig. 7. Laser-welded panel with filling [7].

The panel's internal space between two shell plates can be also used as a channel for cables or tubes widely applied in ship construction. The cables or pipes (for drink water or sewage system, heating equipment, etc.) placed inside can be fixed directly by the panel filling, so that fixing elements are not necessary.

## MODULAR SECTIONS BUILT OF LASER-WELDED PANELS

To form bigger sections of ship structure, connection of some panels is necessary. The panel - panel connection in the plane parallel to the stiffeners (see Fig.8) is less critical in comparison to that in the plane perpendicular to them because in the other case load is transferred only by the relatively thin shell plates.

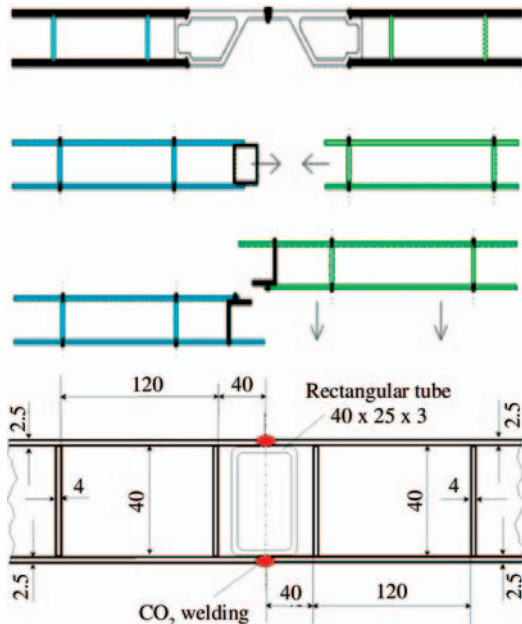


Fig. 8. Ways of making panel -panel connection in the plane parallel to the stiffeners [8].

Such prefabricated sections are then used as – for instance – deck construction or transverse and longitudinal walls (bulkheads) of ship hull. Fig. 9 (up part) shows a deck construction with T - girders put - on, and prior - installed tubes. The down part of Fig.9 shows a ship interior with walls erected from sandwich panels. The modular character of the sandwich panels makes arrangement process easy and significant labour saving possible because the almost deformation-free sandwich elements constitute basically post-treatment-free modules.

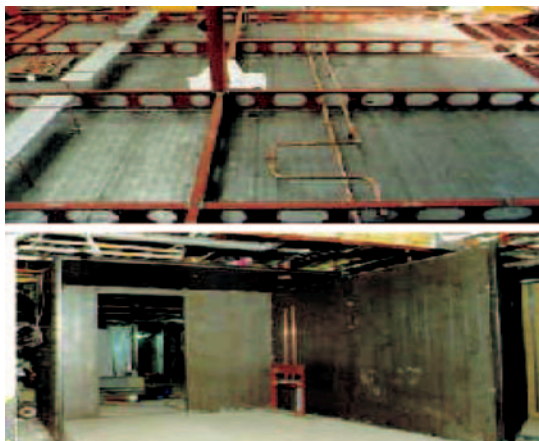


Fig. 9. Deck and wall sections made from laser-welded panels [9].

The smooth surface of the panels can be painted without additional preparation and does not need any additional covering.

## HYBRID STRUCTURES

The structure which contains both conventional and laser-welded components is called *hybrid* structure. The using of laser-welded sandwich panels often requires – (e.g. in bow or stern area of ship deck) that the panels have to be combined

with the conventional structures. To this end additional joining elements are also necessary. A typical hybrid construction is presented in Fig.10.

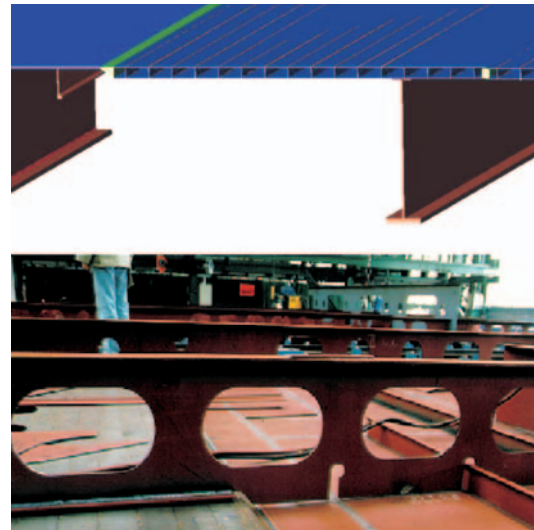


Fig.10. Example of a hybrid structure [10].

Due to the fact that at the moment any rules for application of such structure do not exist, each particular design has to be subjected to a separate evaluation. However on the basis of the results of certain research investigations it is possible to formulate some general principles related to sandwich structures – see Fig.11. Every concentrated load applied to sandwich structure should be introduced rather into a stiffener than non-supported plate area to avoid a local failure. Otherwise – a local strengthening in such points is necessary.

The rigid fixing of panel edges leads to a smaller value of global deflection than that in the case of their simple supporting. Connection of sandwich panel and conventional structure always creates a high - stress region.

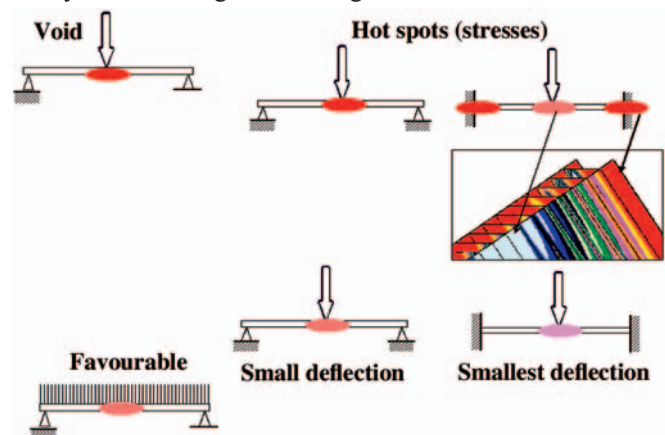


Fig.11. Strength problems regarding sandwich structures [11].

Problems of the joining two sandwich panels and a sandwich panel with a conventional structure have been presently subjected to intensive studies.

## SUMMARY

Laser-welded panels constitute innovative modular components which already have found application to ship structures. They are characterized by considerably greater stiffness at the same mass, as compared with conventional structures, and they are easier in assembling.

Effectiveness of the hull structure assembling process can be considerably improved by using sandwich elements when the still open organizational and strength problems are solved.



**BIBLIOGRAPHY**

1. Metschkow B., Graczyk T.: *Laser welded joints in shipbuilding*, Marine Technology II, proc. of the Second International Conference on Marine Technology Odra'97, Szczecin, 13-15 May 1997, ed. Computational Mechanics Publications - Southampton & Boston, 1997.
2. Meyer Shipyard: *Ships built by light beams*, [http://www.schulergroup.com/en/40applications/20Laser\\_Technology/30gross\\_und\\_dickblechbearbeitung/Inform\\_Meyer\\_Sonderdruck\\_englisch.pdf#search=%22%2Bmeyer%2Bshipyard%22](http://www.schulergroup.com/en/40applications/20Laser_Technology/30gross_und_dickblechbearbeitung/Inform_Meyer_Sonderdruck_englisch.pdf#search=%22%2Bmeyer%2Bshipyard%22)
3. <http://www.meyerwerft.de/main.asp?what=yard&id=612>
4. Elenbaas M., Reinert T., Gosch T.: *Sandwich Technologies In Marine Applications*, Sandcore, [http://www.sandcore.net/bal\\_ims\\_controler.php?menu=YjdmMjE1OztmZmdiM2piPw=&publication\\_id=MmRkMGZq](http://www.sandcore.net/bal_ims_controler.php?menu=YjdmMjE1OztmZmdiM2piPw=&publication_id=MmRkMGZq)
5. Kujala P., Romanoff J., Tabri K., Ehlers S.: *All Steel Sandwich Panels – Design Challenges for Practical Applications on Ships*, 9th Symposium on Practical Design of Ships and Other Floating Structures Luebeck-Travemuende, Germany © 2004 Schiffbautechnische Gesellschaft e.V.; [http://www.tkk.fi/Units/Ship/Publications/esitelmat\\_eng.html](http://www.tkk.fi/Units/Ship/Publications/esitelmat_eng.html)
6. Thomas Reinert : *Laser Welding and I-core® Panels*; Sandwich-Präsentation-V6. 29-04-2002
7. Boon B.: *Metal sandwiches in ships*. Bart Boon Research & Consultancy, <http://www.sandcore.net/>
8. Roland F., Reinert T.: *Laser Welded Sandwich Panels for the Shipbuilding Industry*; USER GROUP Inauguration, Advanced composite sandwich steel structure Bremen 19.09.2000, <http://sandwich.balport.com/usergroup.htm>
9. Blomquist P.: *Precision Light Systems* NSRP SP NSRP SP-7 Meeting April 5,2006 [http://www.nsrp.org/panels/weld/downloads/040506\\_PLS\\_LaserFab.pdf#search=%22%22Precision%20Light%20Systems%22%20Blomquist%22](http://www.nsrp.org/panels/weld/downloads/040506_PLS_LaserFab.pdf#search=%22%22Precision%20Light%20Systems%22%20Blomquist%22)
10. <http://www.meyerwerft.de/main.asp?what=yard&id=1269>
11. Author's figure



Photo: Janusz Kozak

*Versatile stand for strength tests of natural scale ship hull units,  
Faculty of Ocean Engineering and Ship Technology, Gdańsk Technical University .*



# Problems of strength modelling of steel sandwich panels under in-plane load

Janusz Kozak, D.Sc., Eng.  
Gdańsk University of Technology



## ABSTRACT

Paper presents examples of laboratory test and numerical modelling results of steel sandwich panels under in-plane load. Test and modelling procedure is presented and comparison of numerical and laboratory test obtained results of static compression is discussed.

**Keywords** : laser weld, laboratory test, strength properties, in-plane load

## INTRODUCTION

Rapid development of new technologies, which is observed during last several years have made impact also on shipbuilding structures. Some new materials and new manufacturing techniques have been developed. Among other new ideas, the laser welding techniques start to find their position as alternative methods of joining components of ship structure. Such capabilities create new opportunities of changing the configuration of typical ship structure : instead of the “classical” design consisted of shell plating supported by a grid system of heavy stiffeners one can imagine a design similar to that already applied in glass reinforced plastic structures, namely two shells connected by an internal system of thin stiffeners (webs). This is the idea of sandwich structure – steel or aluminium panels manufactured from two shell plates of 3-4 mm thickness , internally supported by one directional system of stiffeners of about 40 mm in depth, with all components connected by laser welding, Fig.1.

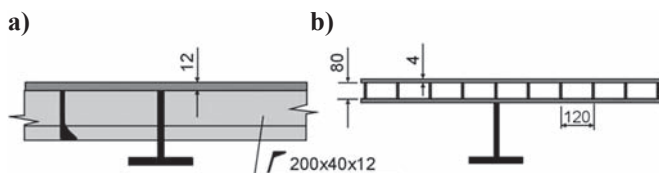


Fig. 1. Ship deck structure of: (a) conventional design (b) sandwich design .

Application of such new structure requires to determine its characteristics by taking into account its strength, corrosion, vibration, fire protection and fatigue properties, in order to get approval – from the side of classification societies – that they are not worse as compared with those of the classical structure. Majority of such parameters are usually obtained from the laboratory tests carried out on models or full-scale structures.

The application of the structure as in Fig.1b in place of the conventional design (Fig.1a) can provide weight reduction by at least 34% and reduction of the manufacturing costs by about 50% [2].

## LABORATORY FULL - SCALE TESTS

Ship hull during its service life is subjected to various loads and their combinations : global, regional (zone) and local. Global loads affects the whole ship hull structure causing its bending or torsion which generate loads acting – among others

– in planes of decks, bottom shell plating or longitudinal and transverse bulkheads. Compressive stresses can lead to buckling of thin shell plates, pre-deformed during manufacturing process. Due to the fact that the shell plating in sandwich structure is significantly thinner than that in conventional structure one can expect higher sensitivity of sandwich structure in regard to buckling phenomena.

A program of laboratory tests of full - scale sandwich panels was elaborated and performed in order to determine basic characteristics of the steel sandwich structure behavior under in-plane load and – further – to formulate and verify analytical formulae for its proper dimensioning. To determine stiffness characteristics of models in relation to their geometry and manufacturing deformations, the family of 3000 x 500 mm models were designed with taking into account some combinations of the model depth, shell plating thickness, core structure and internal filling, as shown in Fig.2.

For the applied combination of cross-section properties, two core geometries were selected : plate stiffeners (webs) perpendicularly placed against shell plating (I-core) and corrugated webs (V-core), Fig.2. For I-core panels the uniform spacing of 80 mm between stiffeners and their thickness of 4 mm was applied, for V-core – the 2 mm constant thickness of stiffeners was chosen. The axial compression tests were performed on a versatile static/fatigue testing machine of the compressive load capacity up to 4000 kN. A set of joints was used to properly exert and distribute the in-plane load into tested model. Such joints make it possible to apply evenly distributed pure axial forces to both edges of the model. This idea is illustrated in Fig.2. Prior to loading, initial deformations of each of the models were precisely measured.

During the test each of the models was subjected to a compression load step-by-step increasing till the moment of complete loss of load-carrying capacity of the model. At each level of the applied load, strain and displacement measurements by means of appropriate gauges were carried out. It was observed that failure mode of tested models is dependent on their cross-sectional geometry, i.e. type of core, shell plating thickness and depth of stiffeners. The failure modes varied from the whole - model ”global” bending without any loss of stability of compressed shell plating - through the “global “ buckling, i.e. loss of stability of the whole compressed shell plating – to the “local” buckling, i.e. loss of stability of the whole cross-section of the model in its middle part; the last model presented failure modes dependent on geometrical properties. Fig.3 illustrates the above mentioned failure modes.

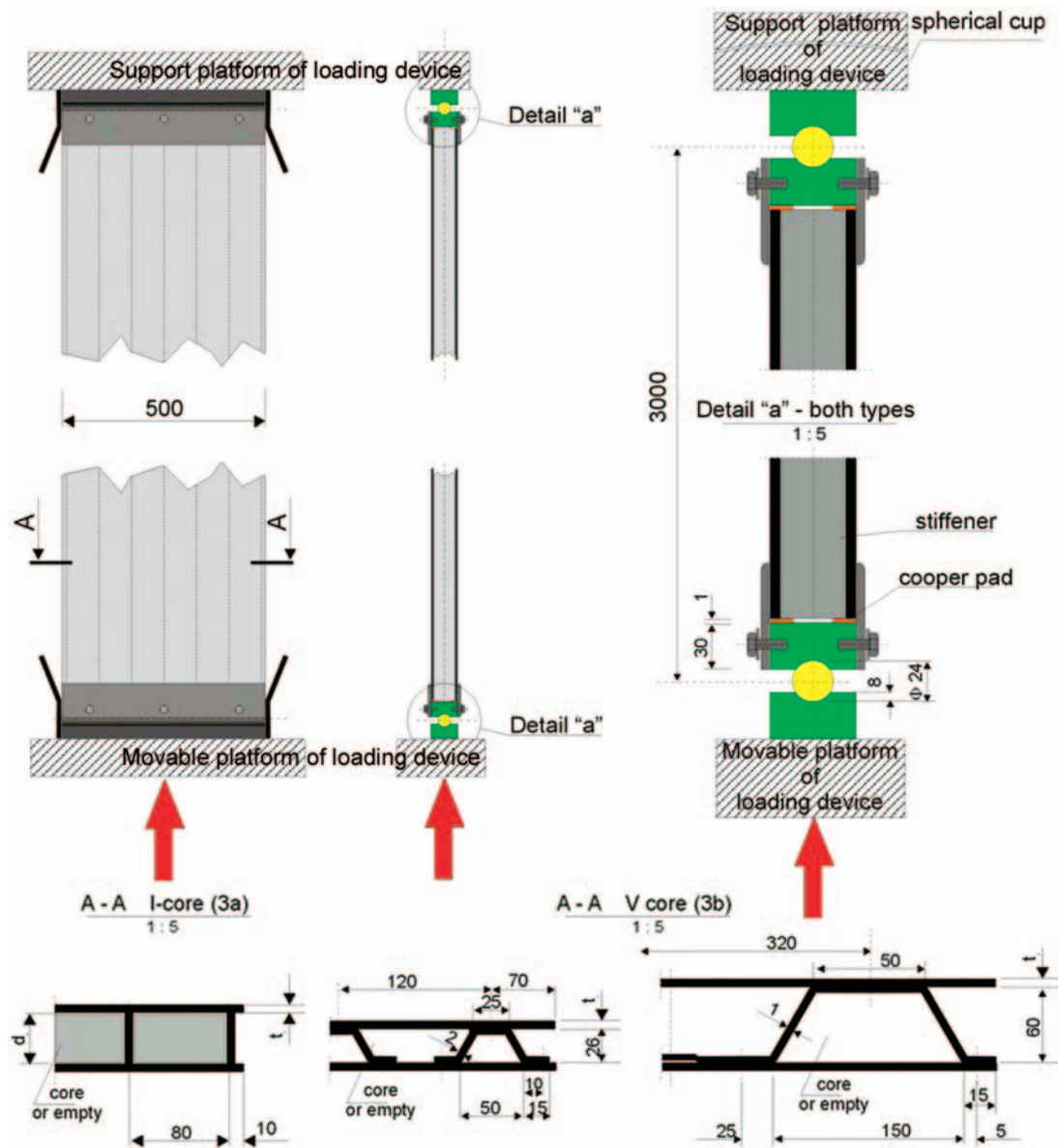


Fig. 2. In-plane load geometry and loading scheme of the tested models.

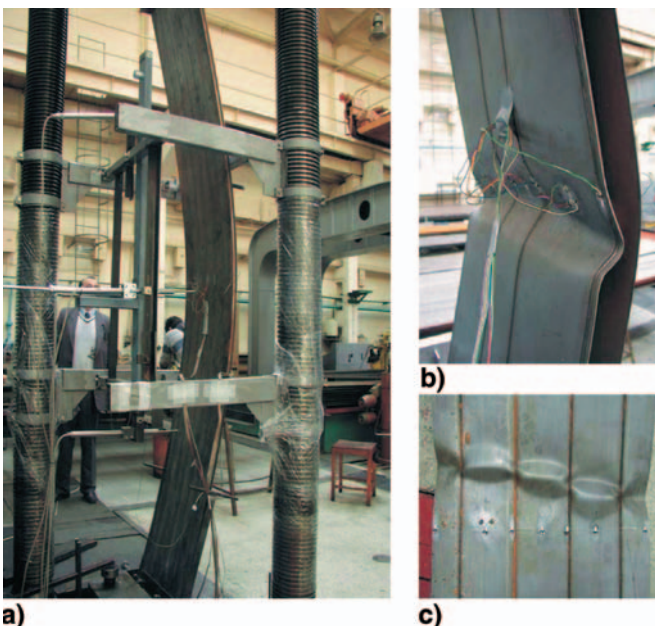


Fig. 3. "Global" bending failure mode: a) pure bending, b) global buckling, c) local buckling.

After systematisation, the tests results showed that two general failure modes can be distinguished. Fig.4 presents the relationship of nominal compressive stresses and longitudinal displacement. Models of certain geometries showed the typical "buckling" curve with almost linear load-displacement characteristics up to critical load level and a subsequent sudden

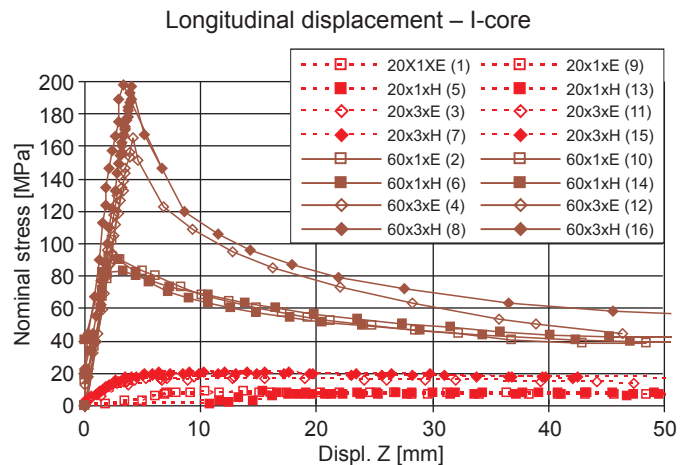


Fig. 4. Results of static compression test of the model of I-core geometry.



collapse; such behaviour is characteristic for the models with high - depth stiffeners, and – to a smaller extent – depending on shell thickness. Models of some other geometries presented the “global bending”, i.e. the behaviour characterized by a smooth load - displacement relationship.

The following notation was used to describe each of the models :

for example – 20x1xE stands for : “20” – stiffener depth of 20 mm, “1” – shell plating thickness of 1mm, “E” – no filling material , i.e. “ Empty” model, and alternatively “H” – high density core (balsa wood).

It was observed that the failure modes of the tested models were strongly influenced also by initial deformations which usually occur in every welded structure as a result of the manufacturing and transport processes.

### NUMERICAL MODELLING

On the basis of the previous studies on behaviour of laser-welded T-joint [1] it was assumed that the numerical modelling of sandwich structure should be done very carefully to reflect its particular properties. To this end, SOLID186 finite element from ANSYS library, was applied. It is 20-node solid element of quadrilateral shape function and three degrees of freedom in each nodal point (UX, UY, UZ). To the presented calculation the variant of 14 integration points was applied. Fig. 5 presents the whole model and a detail of precise mesh in the laser weld region. Due to symmetry of the analysed body, only 1/4 of the real structure was modelled. In order to reflect particularities of the joint the real width of laser weld as well as a gap between stiffener and shell plate was modelled.

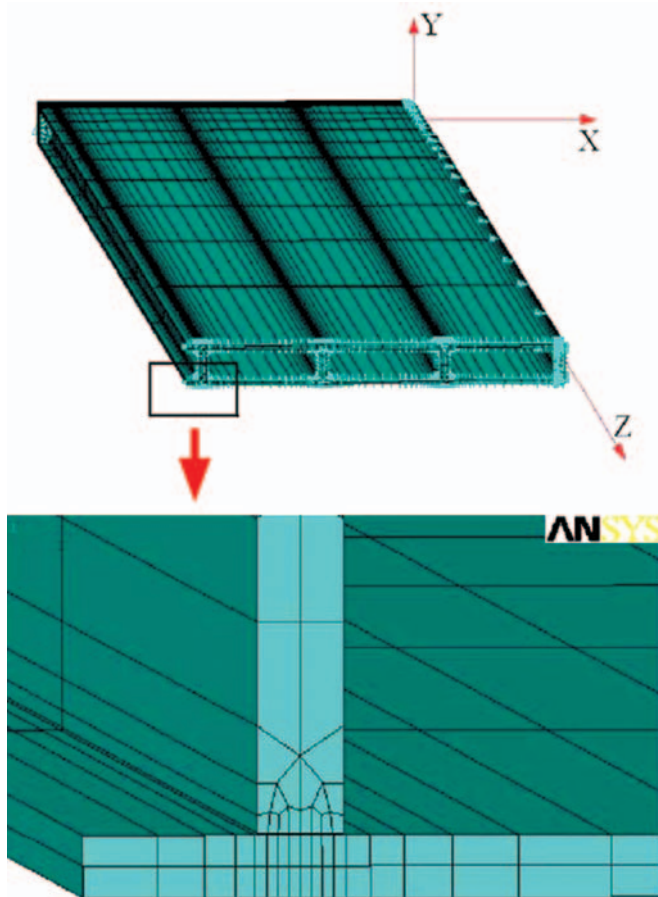


Fig. 5. Numerical computation model and detail of its mesh .

Stress distribution image resulting from the example calculations (Fig.6) confirms the fact of collaboration of shell plating and stiffeners in the compressed region of the failed structure. Such phenomena underline the importance of proper modelling in this region.

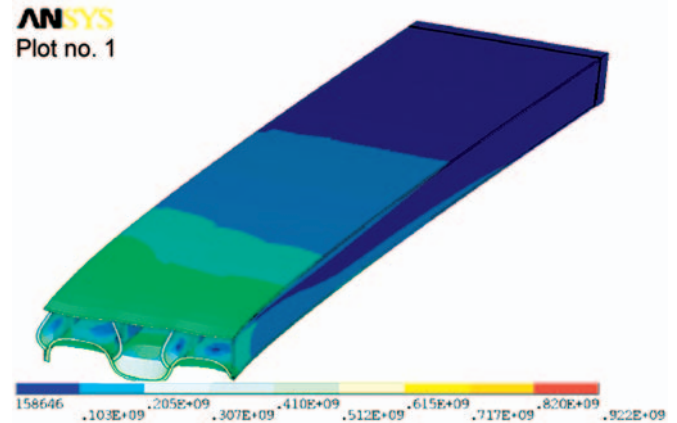


Fig. 6. Stress distribution in shell plating and stiffeners .

The comparison between results of numerical calculations and laboratory tests (Fig.7) shows that the maximum calculated load carried by the analysed structure is lower than that recorded during the real full-scale model test. This difference is probably caused by the fact that the numerical model reflects only the bending of the laser weld. Contact phenomena which occur in the real structure was not modelled at all.

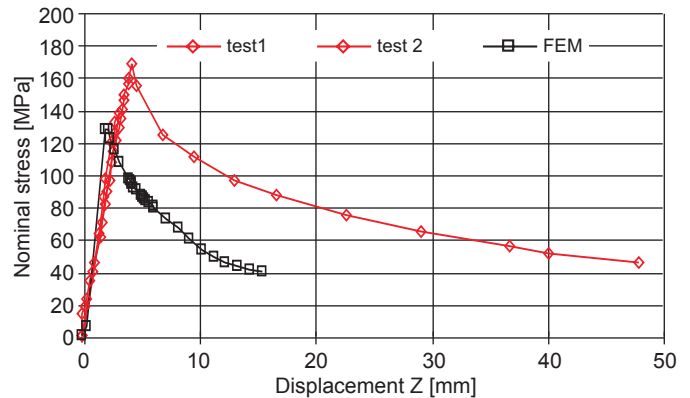


Fig. 7. Comparison of the results obtained from numerical calculations and laboratory tests .

### CONCLUSIONS

A series of full-scale steel sandwich models was tested under in-plane compression load. The models having the same dimensions varied by geometrical properties of their cross-section as well as core material density. During the tests the load - response relationships of the models were investigated and recorded.

The combined effect of stiffener depth and filling material was also observed. For different geometrical properties the effect of the filling material is complex and stronger for lower values of shell plating thickness.

However it was observed that the stiffener depth and shell plating thickness influence the stiffness of the structure considerably stronger than the presence of filling material and its density.

The tests indicated that failure mechanism (mode) depends on geometrical properties of model’s cross-section – especially

on the ratio of stiffener depth and shell plating thickness. The observed failure mechanisms (modes) were as follows :

- ❖ global bending of the whole model
- ❖ global loss of stability of the whole compressed shell plate
- ❖ local damage of model's cross-section due to a combined loss of stability of compressed shell plate and adjacent parts of stiffeners.

From the qualitative comparison of I-core and V-core geometry of stiffeners it results that I-core stiffener system has more favourable properties regarding in-plane-load response characteristics.

Manufacturing deformations considerably affected the load-displacement characteristics of compressed model. This is one of the most important parameters affecting the buckling characteristics of steel sandwich panel; hence establishing appropriate accuracy tolerances for manufacturing the panels and maintaining the final product within the assumed accuracy limits is crucial for reaching the proper buckling strength of panel.

The numerical modelling of the laser-welded steel sandwich structures should be very carefully performed and its results

should be dealt with a caution because of particular properties of laser-welded joints as well as a sensitivity of real structure to presence of manufacturing deformations.

### *Acknowledgements*

This paper is based upon results of the work carried out within the frame of the following EU research projects: “**Advanced Composite Steel Sandwich Structures**” – SANDWICH, G3RD-CT2000-00256, “**Coordination Action on Advanced Sandwich Structures in the Transportation Industry** – SAND. Core, TCA3-CT-2004-506330 and “**Application of Steel Sandwich Panels into Ship Structure**” – ASPIS, EUREKA E!3074.

### **BIBLIOGRAPHY**

1. Boroński D., Kozak J. : *Research on deformations of laser welded joint of a steel sandwich structure model*. Polish Maritime Research, No2, 2004
2. Roland F., Metschkow B. : *Laser Welded Sandwich Panels for Shipbuilding and Structural Steel Engineering*. Information materials of Meyer Werft

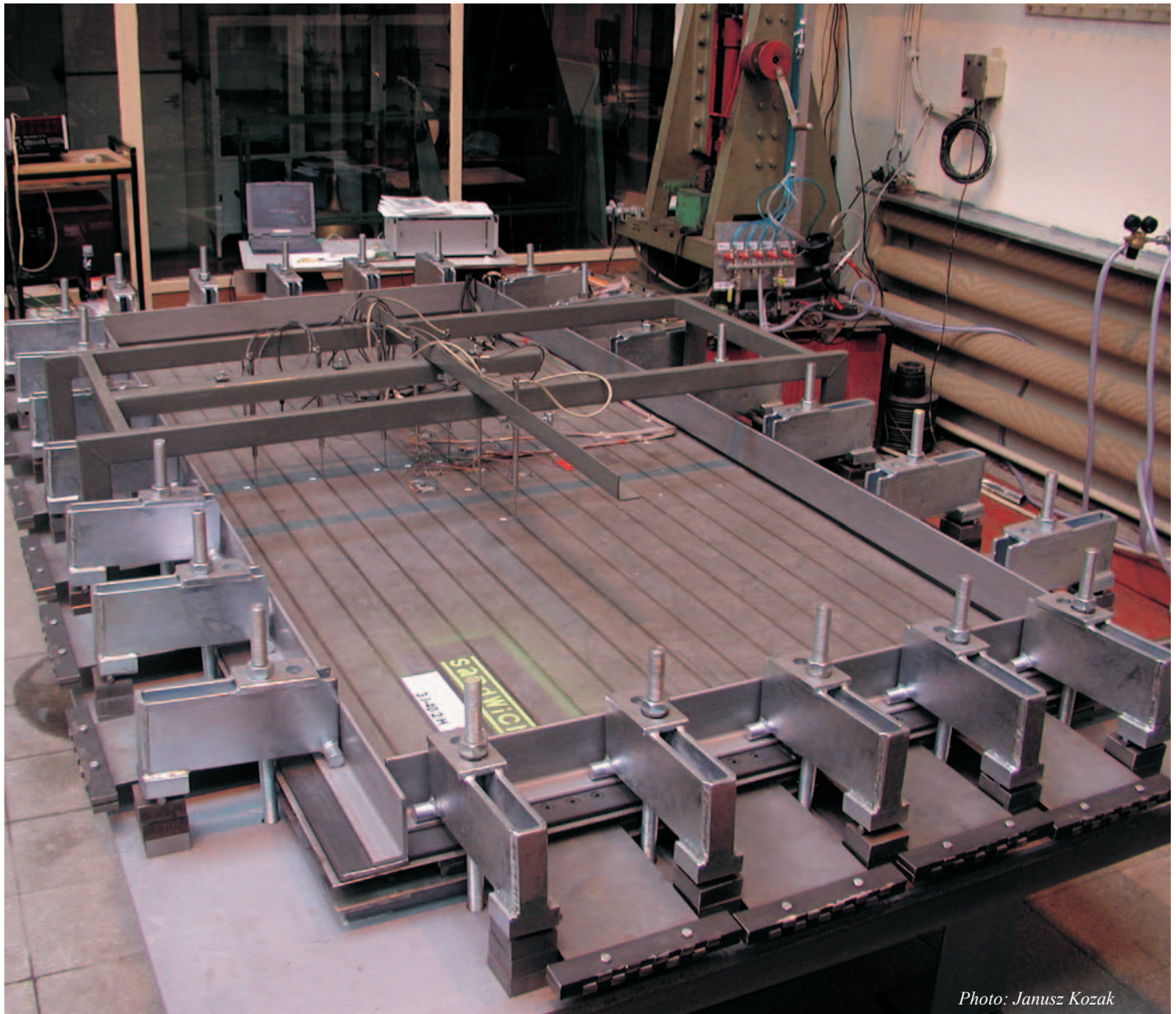


*Photo: Janusz Kozak*

*Sandwich panel during test under water pressure loads .*



# Fatigue life of steel laser-welded panels

Janusz Kozak, D.Sc., Eng.  
Gdańsk University of Technology



## ABSTRACT

*This paper presents a proposal of algorithm for determining fatigue life of steel laser-welded panels, elaborated on the basis of results of the author's laboratory tests of full-scale structural models. The methodical algorithm and an example of elaborated design curve is presented.*

**Keywords :** laser weld, laboratory test, strength properties, fatigue of structure

## INTRODUCTION

The idea of replacement of the classical ship hull structure – developed for centuries – by a novel thin double - shell structure having most of its internal members contained inside it, emerged in the end of the 1950s, however serious interest to it was only paid by US Navy which introduced LASCOR panels as late as in the end of the 1980s. The most spectacular example of this application has been the design of aerial platform for USS „Mt. Whitney”, which has made it possible to decrease the weight of the high-placed structure by 9 t. It significantly contributed in improving the ship's stability, Fig.1.

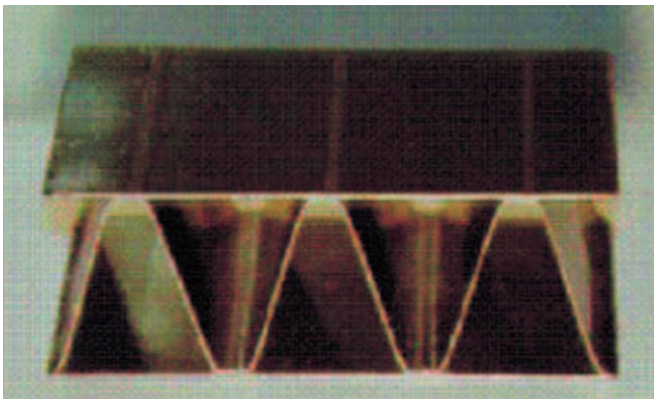


Fig. 1. The aerial platform made of LASCOR panel .

In order to ensure fulfillment of safety conditions for total assumed service time the conditions should be verified with taking into account the criteria associated with structural strength, corrosion protection and fire resistance. For the classical ship steel structure the criteria have been developed for a few dozen of years and they now form a systematically verified set of relevant requirements issued by ship classification societies. Their guidelines and recommendations dealing with the assessment of fatigue life of hull structures are one of the latest and still developed groups of the requirements of the kind.

## THE AUTHOR'S RESEARCH ON FATIGUE QUALITIES OF SANDWICH MODELS

In contrast to the classical welded steel structures the problems – especially those dealing with strength – associated with the application of novel solutions such as steel double-shell complex sandwich structures, have been investigated so far to an insufficient extent. In particular the fatigue strength problems of such structures have started to be recognized and investigated as late as in the last years. Whereas every application of novel solutions of ship hull strength structure requires to have at one's disposal relevant analytical procedures including those concerning fatigue life assessment. Such procedures for steel sandwich panels are still lacking.

The algorithms successfully used in shipbuilding, elaborated for classical structures, have not been so far positively verified to be used in sandwich structures because of their different features and lack of research data.

Hence an attempt has been made to elaborate a procedure for estimation of fatigue life of such structures within the frame of the research programs financially supported by European Union, in which the Faculty of Ocean Engineering and Ship Technology, Gdańsk University of Technology, has taken part. In the frame of the research program, behaviour of steel sandwich structures in various versions of geometry, boundary conditions and load configuration, were tested under variable load.

### *Tests of the models having 3000x1500 mm overall dimensions, („a” type)*

The fatigue tests were performed under concentrated load applied in the centre of the model rigidly restrained at all its edges. The test stand and the model itself is shown in Fig.2.

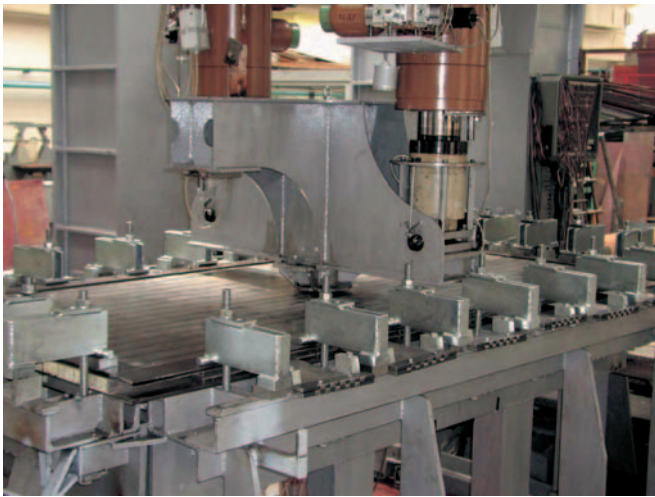


Fig.2. The model „a” under fatigue testing .

In the fatigue tests in question load levels were selected on the basis of their calibration with the use of successive static load tests during which signals from strain gauges placed on both shell plates, were recorded.

When tested, the models were loaded by cyclic constant-amplitude load of about 4 Hz frequency and the stress ratio R equal to about 0.1.

Fatigue cracks appeared in the transition zone between the face of weld and original material of the shell plate under tension. The cracks always appeared just under the middle web. However in two cases the cracks of a similar character appeared also under third web, counting from the mid-span of the model. In all the cases the cracks were caused by the tensile stresses in the shell plate, acting perpendicularly to the course of the weld. In Fig.3 is shown the crack occurrence area and in Fig.4 – a fractographic image of the crack surface.



Fig. 3. Fatigue cracks in the model .

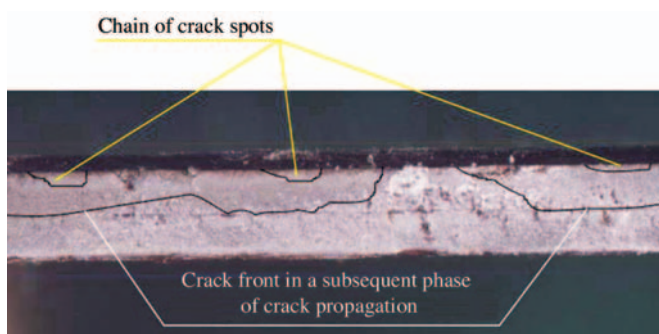


Fig. 4. Fatigue crack surface .

A macro-fractographic analysis revealed the presence of a chain of tiny fatigue spots on the crack surface. This confirms that the material structure within the crack zone uniform and there is no clearly weak points of the kind of welding defect.

### Tests of the models having 1000x500 mm overall dimensions, („b” type)

The models having the same cross-sectional geometry as in the preceding case, were loaded by a concentrated cyclic load applied in the mid-span of the model freely supported along its longer sides.

In the tested models the failure process – regardless of a level of applied load – progressed in the same way : fatigue crack was initiated in the laser weld joining the extreme web with the shell plating in the vicinity of the web’s end and it next propagated along the web towards the model centre, Fig.5.

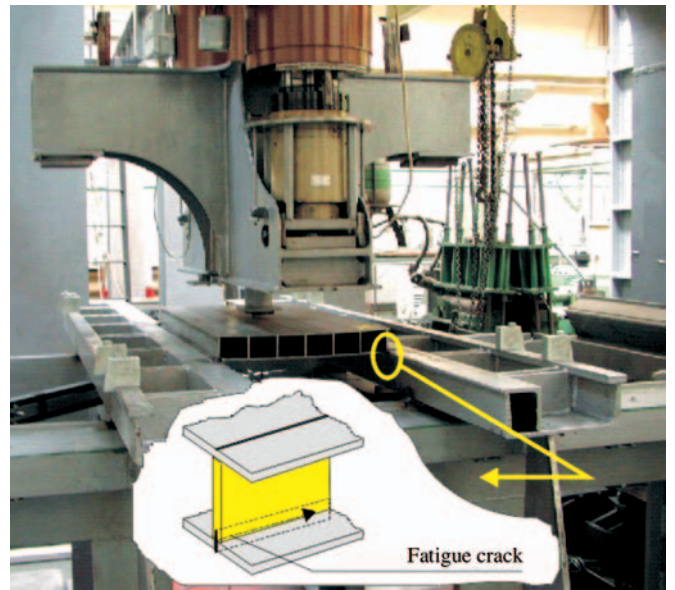


Fig. 5. The way of progressing the failure process in the tested „b” models .

### Tests of models of joints

Some solutions of the joints were also tested, the same as for the models of the geometry close to that of 3000 x 15000 mm models. During the tests, in the sandwich structure on its shell plating surface appeared the cracks initiated in the laser weld and propagating perpendicularly to the course of the weld, Fig.6.

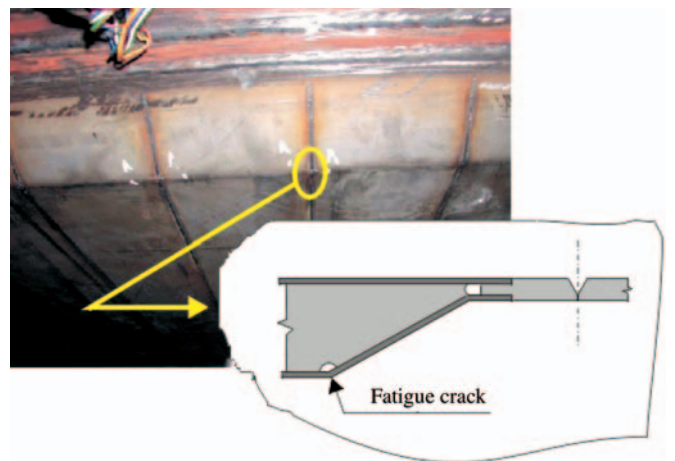


Fig. 6. Crack in the model under testing .



## A PROPOSAL OF THE PROCEDURE FOR FATIGUE LIFE CALCULATION OF STEEL LASER-WELDED PANELS

Taking also into consideration results of other investigations of this author [1,2,3] one can state in a more general way that in the laser-welded double-shell panels of the webs perpendicularly placed to the shell, one out of the following five cracking models can occur, depending on a type of structure geometry, applied loading and supporting mode, see Fig.7. :

- ★ 1<sup>st</sup> – a crack appearing in the tensioned shell plating in the zone of laser weld penetration, pointing the direction perpendicular to the weld axis, caused by tensile stresses resulting from global bending of the panel
- ★ 2<sup>nd</sup> – a crack appearing in the tensioned shell plating in the laser weld, and next in the shell plate material, pointing the direction perpendicular to the weld axis, caused by tensile stresses resulting from global bending of the panel
- ★ 3<sup>rd</sup> – a crack appearing in the tensioned shell plating, caused by local tensile and shear stresses (such a state should not appear in a properly designed structure)
- ★ 4<sup>th</sup> – a crack appearing in the laser weld in the region where shell plating and end surface of adhering web contact to each other, caused by the weld bending resulting from mutual rotation of the web and adhering strip of shell plating
- ★ 5<sup>th</sup> – a crack appearing in the laser weld in the region where shell plating and end surface of adhering web contact to each other, caused by combined stresses resulting from weld bending and shearing.

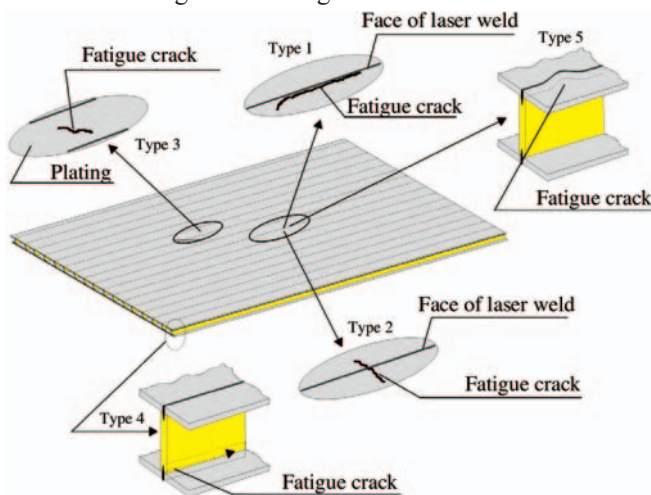


Fig. 7. Cracking models which can appear in steel sandwich structures .

For the classical welded steel structures have been proposed several calculation approaches based either on the concept of nominal stresses, "hot spot" method or deformation criteria, Fig.8 [6].

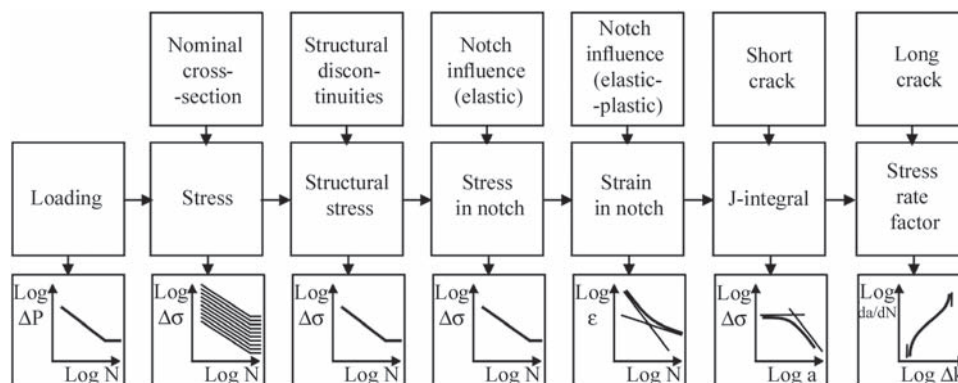


Fig. 8. Some approaches to fatigue strength calculation [6].

For ship structures they are expressed in the form of guidelines, rules and recommendations issued by ship classification societies.

In Fig.9 the interpretation of the nominal, structural (geometrical) and in-the-notch stresses acting in the weld penetration zone, is presented [5].

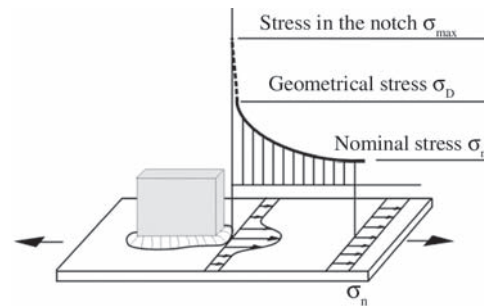


Fig.9. Interpretation of the nominal, structural (geometrical) and in-the-notch stresses acting in the weld penetration zone [5].

The collected results of the investigations make it possible to elaborate procedures for the fatigue life assessment – based on the concept of nominal stresses [4,5] – of the steel laser-welded double-shell panels having their webs perpendicularly placed to shell plating. Such assumption is justified by the fact that the geometry of laser-weld neighbourhood – regardless of full-scale panel dimensions – is always the same. The panels – due to their configuration and internal connections – are obviously much more sensitive to large stresses caused by specific structural features or local manufacturing factors. It could be for instance local deformations of shell plating due to assembling, incorrect transporting or turning in the course of manufacturing process. Initial deformations resulting from laser welds laid non-symmetrically relative to web axis in the course of manufacturing process, constitute a separate problem. Such stress concentrations are random non-predictable phenomena hence during calculation process modelling their influence is not possible. Their influence on fatigue life can be controlled by selecting appropriate manufacturing tolerances and carrying out calculations for the structures initially deformed but still complying with the permissible tolerance limits.

Hence the procedure for fatigue life calculation of steel laser-welded sandwich panel should comprise the following steps :

- ❖ Determination of the field of deformations and stresses
- ❖ Determination of a phenomenon controlling crack development (stress, deformation)
- ❖ Choice of a cracking mechanism (model) and crack occurrence region
- ❖ Determination of a value of the reference parameter for a given cracking model

- ❖ Choice of an appropriate design curve
- ❖ Determination of fatigue life from the chosen design curve.

In order to conduct calculations in compliance with the above proposed approach it is necessary to have at one's disposal a set of design curves for each of the distinguished cracking models shown in Fig.7. The case „4” creates a problem as it seems that for this cracking model crack development is controlled more by deformation mechanism than stress one. For the remaining cases an important factor conditioning the correctness of obtained results is to assume the same reference stresses for the tests from which design curves are determined and for the calculations when the use is made of the curves – as far as both the choice of a stress tensor component and a way of its calculation is concerned.

The design curves as such can be determined on the basis of laboratory tests of elementary models of joints, and the above mentioned uncertainties can be taken into account by assuming an appropriate value of safety factor.

### DESIGN CURVES OF BASIC FATIGUE CRACKING MODELS FOR STEEL LASER-WELDED STRUCTURES

The above postulated necessity of having at one's disposal a set of fatigue design curves for each of the cracking models, based on systematic tests of elementary specimens – which have not been published so far – has constituted a premise to undertake such effort on the basis of own research. In this frame were conducted systematic tests of elementary specimens of a laser-welded joint having its geometry and loading conditions corresponding with the case „1” from Fig.7. Such specimen is shown in Fig.10.

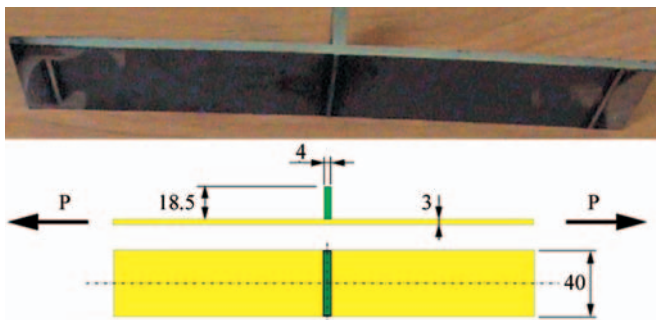


Fig. 10. Geometry of the specimens used for modelling the case „1” (Fig.7).

On the basis of the obtained test results was elaborated a design curve of the slope equivalent to the mean value derived from the results by using the least-squares (RMS) method, and shifted by the value of  $(-2\sigma)$  towards shorter fatigue lives. Such solution guarantees that the fatigue life values calculated on its basis will be achieved with 97.5% probability. The proposed design curve is shown in Fig.11.

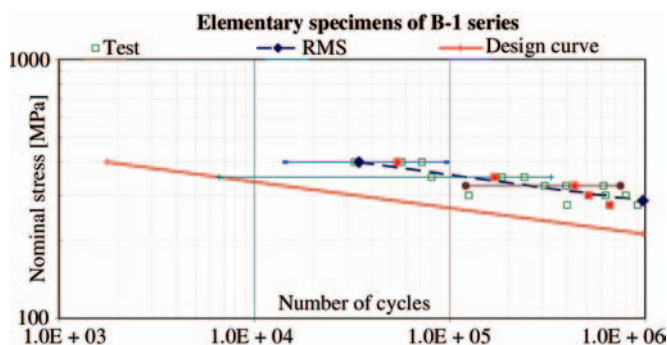


Fig. 11. The proposed design curve for the 1st cracking model.

### CONCLUSIONS

- Steel double-shell laser-welded sandwich panels may constitute an alternative solution for ship hull structures as it offers significant weight and space savings as compared with the classical structures.
- Strength properties of sandwich panels considerably differ from those of ship single-shell structures because of anisotropy of stiffness resulting from their geometrical features, as well as specific properties of laser weld.
- The different properties make possible application of the algorithms for the assessment of fatigue life prepared for single-shell structures, directly to sandwich structures, doubtful.
- On the basis of the full-scale model tests of sandwich panels, performed by the author, the cracking models of such structures subjected to variable loads, were revealed and collected.
- An approach based on nominal stresses was proposed to fatigue life analysis of sandwich panels.
- For the above mentioned approach a design curve based on the test results of an elementary laser-weld joint, was proposed.

The presented results were derived from the work conducted in the frame of the following research projects financially supported by European Union :

- ❖ „SANDWICH” – **Advanced Composite Sandwich Steel Structures** –5<sup>th</sup> EU Outline Program, Contract No. G3RD-CT-2000-00256, 2000-2003
- ❖ “SAND.CORE” – **Coordination Action on Advanced Sandwich Structures in the Transportation Industry**, 6<sup>th</sup> EU Outline Program, Contract No. TCA3-CT-2004-506330 SAND.CORE, 2004-2005
- ❖ „ASPIS” – **Application of Steel Sandwich Panels into Ship Structural Design**, EU research project within the frame of Eureka E!3074 Network, 2003-2006.

### NOMENCLATURE

|  |   |
|--|---|
| a  | – fatigue crack length                    |
| K, ΔK  | – stress intensity ratio and its range    |
| N  | – number of cycles of fatigue load        |
| P, ΔP  | – load and load range                     |
| R  | – load asymmetry ratio                    |
| RMS  | – root mean square                        |
| ε  | – unit strain                             |
| σ, Δσ  | – stress and stress range                 |
| σ <sub>n</sub> , σ <sub>D</sub> , σ <sub>max</sub> | – nominal, geometrical and notch stresses |

### BIBLIOGRAPHY

1. Kozak J.: *Fatigue Properties of Laser Welded Steel Sandwich Panels*. Advanced Marine Materials, Technology & Applications, RINA. London, 2003
2. Kozak J.: *Strength Tests of Steel Sandwich Panel*. PRADS 2004
3. Kozak J.: *Strength tests of steel sandwich panels*. Maritime Transportation and Exploitation of Ocean and Coastal Resources. Proc. of the 12th Int. Congress of the Int. Association of the Mediterranean (IMAM 2005), Lisboa 26-30 Sept. 2005
4. Fricke W.: *Fatigue Strength of Ship Structures*, part I. Germanischer Lloyd. Hamburg, 1997
5. Matoba M., et al. : *Evaluation of Fatigue Strength of Welded Steel Structures – Hull Members*, IIW-XIII-1082-83. 1983
6. Radaj J.: *Review of fatigue strength assessment of non-welded and welded structures based on local parameters*. Int. Journal of Fatigue, No3, 1996



# Strength assessment of a version of joint of sandwich panels

Ryszard Pyszko, M.Sc., Eng.  
Gdańsk University of Technology



*In this elaboration are presented proposals of strength assessment procedure of a joint of two equal-depth sandwich panels so connected in the same plane that the joint line is parallel to stiffeners of the panels. The joint is subjected to lateral and tension loads.*

**Keywords :** sandwich panel, ultimate load-carrying capacity, panel joint

## ABSTRACT

## INTRODUCTION

Searching for novel structural solutions in order to cope with „murderous” pressure of economical factors – so clearly observed in aircraft industry – has not pass over maritime transport. Since in the classical solutions of ship structures continually perfected for centuries not much can be improved one of the ways of the searching for structural improvements is to apply unified structural elements.

Development of laser-welding techniques made its industrial applications possible – and this way – also production of steel sandwich panels being double-skin structures mutually connected by a system of closely spaced stiffeners joined with the plating just by using laser-welding technique. Any introduction of a novel solution into ship hull structure, especially for primary strength members, is associated with the necessity to demonstrate that many requirements, especially concerning structural safety, are satisfied. Some of the structural requirements deal with strength of structural connections among which are also panel-to-panel joints.

## GEOMETRY OF THE ANALYZED JOINT

In the joint in question load is transferred by two external, symmetrical cover plates. The design of the joint together with its geometrical characteristics is shown in Fig.1. The same breadth was assumed for both the cover plates connecting upper and lower plating, respectively. The distance between the panels was so selected as to maintain the spacing between stiffeners of the panels, constant. In the analyzed problem such values of cross-section parameters are searched for at which the joint obtains its maximum load-carrying capacity at :

- ★ a suitable breadth of cover-plate, **dn** - which is associated with its location relative to panel stiffeners (**du** in Fig.1)
- ★ a suitable thickness of cover-plate, **gn** - which is associated with the fillet weld leg (**asp** in Fig.1)

And it is assumed that : the load-carrying capacity of the joint constitutes the possibility of transferring an assumed load by a given structure (joint – connected panels) under condition that neither a loss of structural stability nor extensive plastic deformations of the structure in any its cross-section, occurs. The capacity is related to the assumed value of the stresses,  $\sigma_{red} = f(\text{load})$ , resulting from the applied load.

Description of the geometrical parameters and their denotations (as in Fig.1) are given in Tab.1. Every quantity marked “1” through “15” constitutes the searched variable parameter.

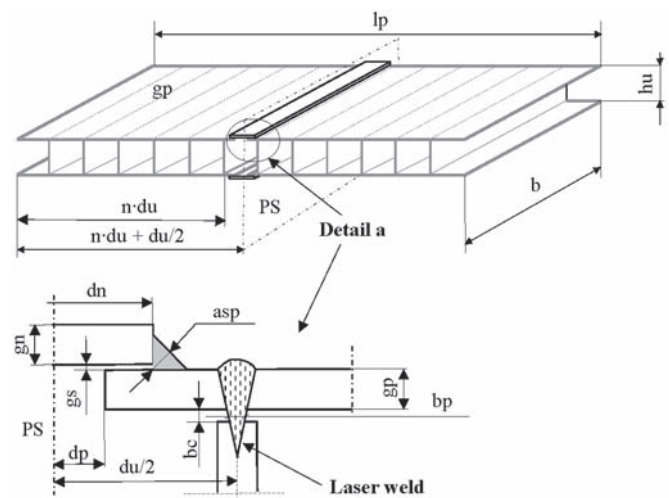


Fig. 1. Geometrical characteristics of the analyzed joint .

Tab. 1. Geometrical parameters of the joined panels .

|                                      |  |
|--------------------------------------|--|
| 1. <b>gp</b> – plating thickness     | 9. <b>b</b> – specimen width                     |
| 2. <b>hu</b> – stiffener depth       | 10. <b>h</b> – total depth of panel              |
| 3. <b>gu</b> – stiffener thickness   | 11. <b>n</b> – number of stiffeners in one panel |
| 4. <b>du</b> – spacing of stiffeners | 12. <b>asp</b> – fillet weld leg                 |
| 5. <b>gn</b> – cover-plate thickness | 13. <b>bp</b> – weld penetration width           |
| 6. <b>dn</b> – cover-plate width     | 14. <b>gs</b> – gap thickness                    |
| 7. <b>bc</b> – gap height            | 15. <b>dp</b> – panel’s end overlap              |
| 8. <b>lp</b> – specimen length       | <b>PS</b> – laser’s plane of symmetry            |

## PROBLEM ANALYSIS

The analysis is aimed at investigation of the behaviour of the considered joint of panels under lateral and tension loading.

### Panel fastening and loading

For the panels in question the following assumptions were taken :

- ⊛ The panel is freely supported at its ends, where one of which is slidable
- ⊛ The load applied to the panel is composed of two sets of forces :  $F_x$  – axial tension forces, and  $F_z$  – lateral forces producing constant bending moment in the region of cover-plate connection – Fig.2. The forces  $F_x$  and  $F_z$  act simultaneously, increase uniformly and independently to each other. The resulting load is a combination of the

forces increasing from zero- value up to that at which the limit load- carrying capacity of the investigated joint is exceeded

- ⊛ Stress distribution at the supports and in the regions of application of forces is of no significance from the point of view of the assumed aim
- ⊛ Geometrical arrangement of the panel together with the cover-plates is symmetrical relative to the plane PS
- ⊛ The load acts symmetrically relative to the plane PS.

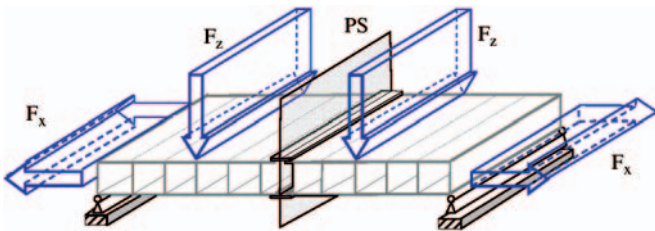


Fig. 2. Loading scheme of PP01 panel.  $F_z$  – pair of the lateral forces producing the constant bending moment  $M_g$  in the region of cover-plate connection  $F_x$  – tensile forces applied to the panel.

### Structural model for FEM calculations

For the above described joint a structural model for calculations by means of Finite Element Method (FEM) was elaborated. With a view of symmetry of the problem as well as the assumed loading mode, some simplifications were introduced as follows :

- simplification of joint geometry (appropriate modeling)
- introduction of appropriate boundary conditions (symmetry)
- application of loads by setting-up appropriate displacements in model mesh nodes.

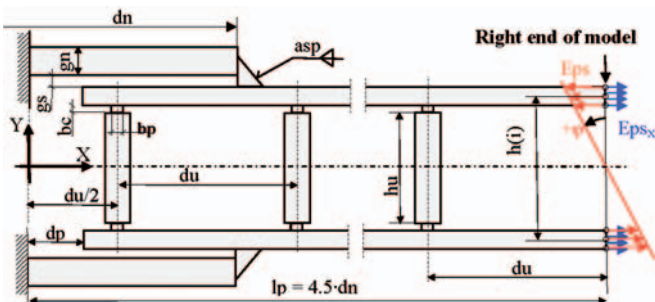


Fig. 3. Geometry of the joint's model for FEM calculations.  $M_g \sim \varphi \sim Eps_\varphi$  – bending moment loading – relevant displacements  $\rightarrow$   
 $F_x \sim Eps_x$  – tension force loading – relevant displacements  $\rightarrow$   
 $h(i)$  – distance between mesh nodes. Remaining notations - see Fig.1 .

The loading onto the joint is realized by applying relevant displacements to the right-hand end of the model, Fig.3, at FEM mesh nodes. The displacements act in one plane and the same directions. Load resultants of the upper and lower plating result from superposition of the displacements  $Eps_x$  and those due to the twisting angle  $\varphi$ , Fig.3.

$$\begin{aligned} Eps(i) &= Eps_x(i) + Eps_\varphi(i) = \\ &= Eps_x(i) + \frac{h(i)}{2} \text{tg}(\varphi) \end{aligned} \quad (1)$$

It was assumed that the displacements along Y – axis, due to the twisting angle, are negligibly small (because of its small values ranging from 0° to 1.2°). Under the above mentioned assumptions the displacement (load) resultants are as follows, Fig.4.

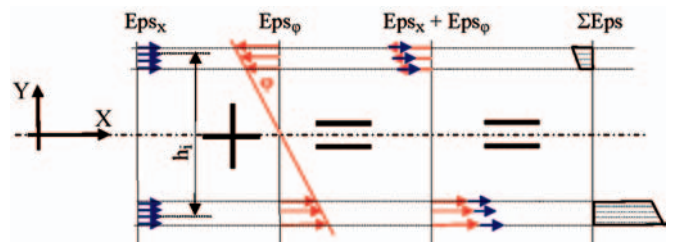


Fig. 4. Load applied to the right-hand end of the model .

In order to find the searched variables the analyzed joint's model was parametrized. The number of the geometrical parameters of the joint was reduced by assuming values of selected parameters constant. The dimensions which can be calculated on the basis of the values of the parameters, were also omitted. The result of the simplifications is presented in Tab.2 ; after the reduction only three searched variables have been left.

Tab. 2. Specification of geometrical parameters describing PP01 joint after simplifications [1]

| Geometrical parameters of the panels to be joined : | Parameters of the panels to be joined, after simplifications : |
|---|--|
| 1. gp – plating thickness = 2.5 mm                  |  |
| 2. hu – stiffener depth = 40 mm                     |  |
| 3. gu – stiffener thickness = 4 mm                  |  |
| 4. du – stiffener spacing = 120 mm                  |  |
| 5. gn – cover-plate thickness                       | 5. gn – cover-plate thickness                                  |
| 6. dn – cover-plate length                          | 6. dn – cover-plate length                                     |
| 7. bc – gap height = 0.2 mm                         |  |
| 8. lp – specimen length = 4.5 du                    |  |
| 9. b – specimen width = 1 mm                        |  |
| 10. h – total depth of the panel = hu + 2(gp+bc)    |  |
| 11. n – number of stiffeners in one panel = 4 pcs   |  |
| 12. asp – fillet weld leg                           | 12. asp – fillet weld leg                                      |
| 13. bp – weld penetration width = 1 mm              |  |
| 14. gs – gap thickness = 0.5 mm                     |  |
| 15. dp – panel's end overlap = 10 mm                |  |

To the assumed model were used the assumptions resulting from a modeling method of sharp notches, which consisted in introducing the under-cuts of suitable values of radiuses, Fig.6.

Also, it was assumed that during load increasing the elements are able to enter in contact. In Fig.6. are indicated the places where the distance between neighbouring pairs of nodes are continuously monitored. After performing the calculations it appeared that – at the initial geometry (for all the considered cases) and the applied mode of model's loading – such contact occurred in a few points only until the model has reached its limit load-carrying capacity - Ngr.

In a limited number of cases such contact occurs in the region 1. The first phase of the sliding contact in the stiffener occurs because of a relatively long distance from the region 1 to the plating support. The instant of the contact is denoted :  $Kr\_posz = nr$ , i.e the number of the step after which the contact will appear. This is illustrated in Fig.5.

A contact in the regions 2 and 3 occurs practically in the phase when the joint itself suffers a damage, i.e. beyond the range where Ngr is determined.



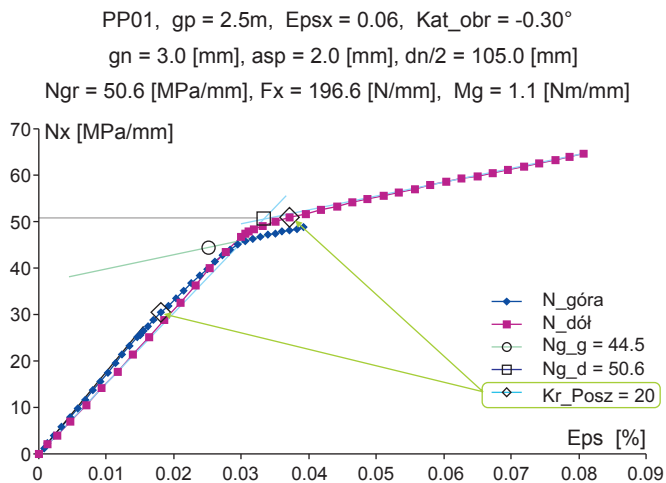


Fig. 5. The diagram of the relation  $N_x = f(Eps)$  with marked loading steps and the contact in the region 1, shown in Fig.6.

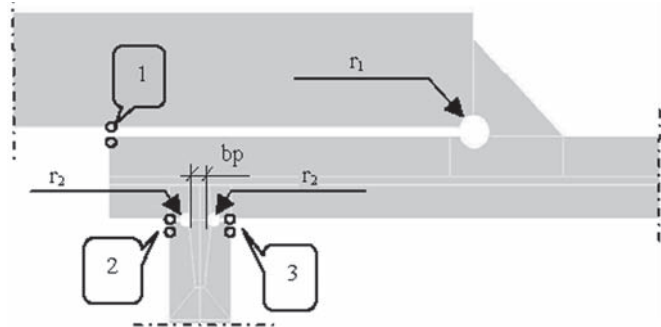


Fig. 6. The detail of FEM model in the region of the cover-plate / panel connection. Fillet weld connection between cover-plate and plating,  $r_1 = 0.8$  mm. Connections between plating and stiffener,  $r_2 = 0.4$  mm. Width of weld penetration :  $bp \approx 1$  mm. Contact regions : 1, 2, 3. Notation of a pair nodes :  $\circ$ .

For the problem in question the linear elastic stress-strain characteristics of material with strain hardening was assumed, Fig.7.

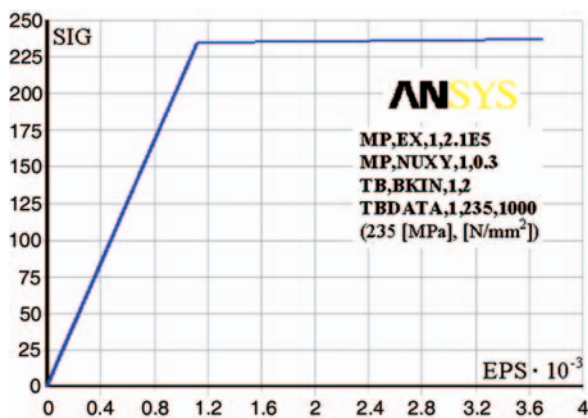


Fig. 7. Stress – strain characteristics of material for plating, stiffeners and welds.

For modeling the structure, the following FEM elements taken from the file of ANSYS software, were used (Fig.8.) :

- ET,1,plane42 – for panel, cover-plates and welds
- ET,2,LINK1 – for contacting element – to maintain constant distance between the ends of panel plates, Fig.7.

**Boundary conditions, Fig.8.**

Because of the geometrical symmetry (Fig.2 and 3) and the mode of load application by means of displacements, Fig.4, the following boundary conditions were used :

```
LSEL,S,LINE,,96
LSEL,A,LINE,,416
Nsl,S,1
D,all,ux,0 ! locked displacements along X- axis
! free displacements along Y- axis
Lsel,all
Nsel,all
Displacements (loading)
```

The displacements are set-up depending on the distance along Y-axis; along X-axis they are applied to the nodes at the right-hand end of the panel, see Fig.3 and 4.

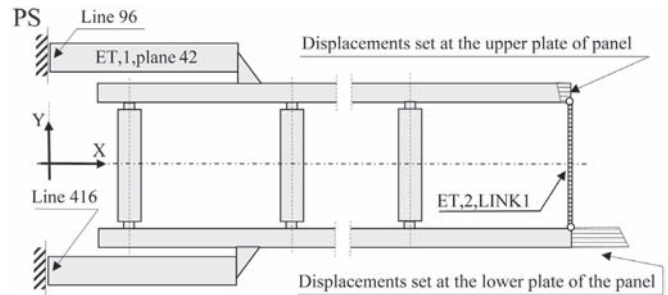


Fig. 8. Model of connections between panel elements, for FEM calculations.

**Calculations – response of the structure**

For the above described geometry, boundary conditions and loading, the calculations were conducted in the range of non-linear material characteristics. The distribution and quantity of reaction forces appearing in the nodes with set displacements, were considered as the response of the structure in question. Next, some simplifications dealing with conversion of the results to their final form, were applied - Fig.9.

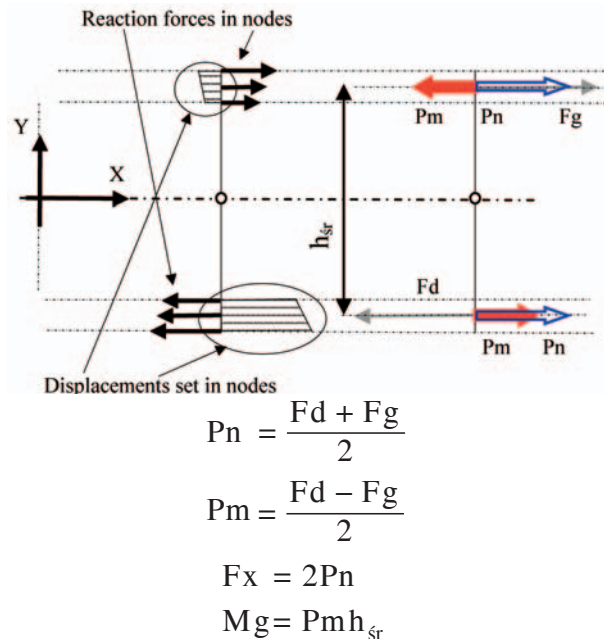


Fig. 9. Determination of the force and bending moment loading the panel.  $P_m$  – pair of forces giving constant bending moment proportional to  $Eps_\phi$ ,  $P_n$  – forces causing tension of the panel, proportional to  $Eps_x$ ,  $F_g$ ,  $F_d$  – resultant response forces in upper and lower plating, respectively.

**Simplification 1** – it was assumed that – due to relatively small thickness of plating as compared with the panel depth – the resultant force in the upper plating,  $F_g$ , and the lower plating,  $F_d$ , can be taken equal to the respective sums of reaction forces in the nodes. The forces mainly act along X-axis, as their components along Y-axis are negligibly small (Fig.9).

**Simplification 2** – it was assumed that the resultant vector of the forces  $F_g$  and  $F_d$  is situated in the middle of the plating thickness  $g_p$  (Fig.9).

**Simplification 3** – it was assumed that at the above given distribution of forces the obtained reaction forces can be converted into the panel loading forces and next into the constant bending moment proportional to  $\varphi$  and the tension force proportional to  $E\epsilon_{sx}$  – Fig.4.

**Analysis of results**

Series of example calculations were performed for the single joint of the PP01 panel of constant geometry and various cover-plate parameters, (Tab.2); the range of variability of the parameters is given in Fig.11. In Fig.10 are shown changes of values of the stresses  $N_x$  in the cross-section where displacements within the panel have been set up, as well as the way of determination of  $N_{gr}$  for the joint in question. In the further part of the analysis the use of  $N_{gr}$  has been deemed more comfortable.

**Eps** – set-up, uniformly increasing load in Eq (1)

**$N_x$**  – stresses along X- axis (response of the structure)

**$N_{góra}$**  – stresses in the upper plating at the right-hand end of the panel, after averaging the reaction forces  $F_g$  (Simplification 2)

**$N_{dół}$**  – stresses in the lower plating at the right-hand end of the panel, after averaging the reaction forces  $F_d$  (Simplification 2).

**Method of tangents** – consists in finding the line tangent to the tension curve at its origin S1- Fig.10 as well as that tangent to the tension curve at its end S2- Fig.10 The intersection point of the tangent lines determines a value of limit stresses for the curve, i.e. those for the cross-section where loads (displacements) have been set up [2].

**$N_{g_g}$**  – value of limit stresses determined for the upper plating– acc. the method of tangents

**$N_{g_d}$**  – value of limit stresses determined for the lower plating– acc. the method of tangents.

Lp. 5,  $g_p = 2.5m$ ,  $E\epsilon_{sx} = 0.06$ ,  $Kat_{obr} = -0.30^\circ$ ,  **$N_{gr} = 49.7$**

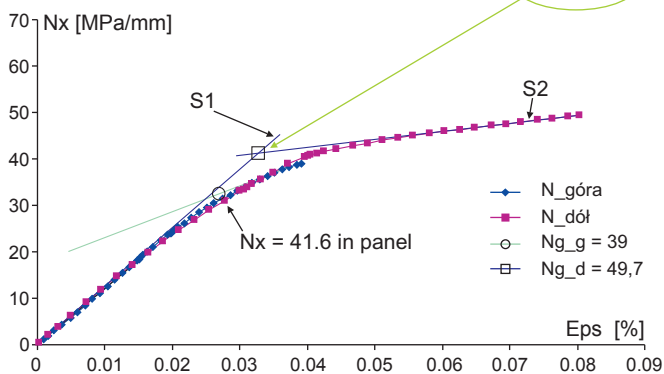


Fig. 10. The diagram of the relation  $N_x=f(E\epsilon_s)$  in the cross-section where the displacements were set at the right-hand end of the panel.

**$N_{gr}$**  – limit load-carrying capacity of the panel, determined by the greater value out of  $N_{g_g}$  and  $N_{g_d}$ . An exceedance of the loads which generate stresses equal to  $N_{g_g}$  (Fig. 10.) does not cause the load-carrying capacity of the panel to be exhausted. Only when  $N_{g_d}$  is reached the load-carrying capacity of the panel is exhausted due to occurrence of plastic deformations in a cross-section, or loss of structural stability, or – alternatively – due to occurrence of both the phenomena simultaneously.

**$g/d$  [krok]** – in this column is given the calculation step in which  $N_x=41.6$  [MPa/mm] Fig. 10 i.e.  $N_{gr} > N_x$ . At the so

determined limit load-carrying capacity, stresses in the panel will be always at the safe side. Moreover, some margin of the capacity, resulting from the difference :  $N_{gr} - N_x$ , is still left.

**$F_x_g$**  – stands for the reaction force in the upper plating in  $g/d$  [krok] step.

**$F_x_d$**  – stands for the reaction force in the lower plating in  $g/d$  [krok] step.

**$F_x$  [N/mm]** – stands for the loading force applied to the panel, Fig.9.

**$M_g$  [Nm/mm]** – stands for the loading moment applied to the panel, Fig.9.

**SUMMARY AND CONCLUSIONS**

The common conclusions for the selected series of the investigations of  $N_{gr} = f(dn, g_n, asp)$  are presented in Fig.11.

- In the case when the values of the cover-plate thickness  $g_n$  are close to that of plating,  $g_p$ , the load-carrying capacity of the joint of the panels maintains nearly on the same level. The fillet weld leg  $asp$  is associated with the cover-plate thickness, Series I, Fig. 11
- The cover-plate length decisively improves the joint's capacity when  $dn > du$ , otherwise it does not show any influence, Fig. 11
- The range of optimum values of the cover-plate length is located outside the first stiffener, within the distance from  $1/4 du$  to  $1/3 du$
- In the cases where values of the cover-plate thickness  $g_n$  are significantly greater than that of the plating thickness  $g_p$ , the joint's capacity increases. This is additionally dependent on the cover-plate length  $dn$  – Series II and III, Fig.11
- The distance  $dp$  should tend to  $dp = du - 1/2 g_u$ , Fig.3
- Because of the limitations of the applied method it was not possible to indicate either a location or cause of exhausting the panel's load carrying capacity. With the use of the applied procedure it is possible to determine  $N_{gr}$ , i.e. the instant when an exhaust of the panel's load-carrying capacity may be expected.

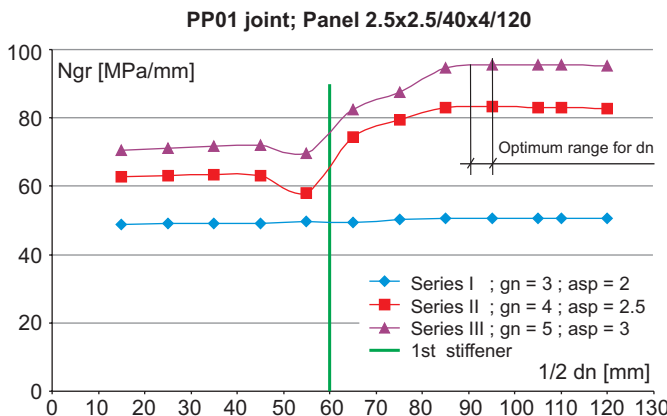


Fig. 11. The diagram of the relation  $N_{gr} = f(dn, g_n, asp)$ .

**BIBLIOGRAPHY**

1. R. Pyszko : *Proposal of a catalogue of joint units of the panels whose stiffeners are to be connected, and the analysis of their manufacturing feasibility* (in Polish). EUREKA: ASPIS E13074 Project, Research report No. 170/E/05. Faculty of Ocean Engineering and Ship Technology, Gdańsk University of Technology
2. Jeom Kee Paik, Anil Kumar Thayamballi : *Ultimate Limit State Design of Steel-Plated Structures*. Jon Wiley & Sons. ISBN 0-471-48632-9.



# FEM analysis of ultimate strength of steel panels

Marian Bogdaniuk, D.Sc., Eng. Gdańsk University of Technology  
 Zenon Górecki, D.Sc., Eng. } IDEK Company Ltd.  
 Mariusz Brzóska, M.Sc., Eng. }

## ABSTRACT

*A method was described of ultimate strength calculation of compressed steel panels proposed for shipbuilding applications. The calculations consist in applying Finite Element Method (FEM) to a model composed of finite shell elements. Large displacement values and plastic flow of material are taken into consideration. Results of ultimate strength calculations of an example panel under compression were compared with those from experimental tests. Accuracy of a proposed simple method of ultimate strength assessment based on the longitudinal bending theory of rod with initial deflections, was also investigated.*

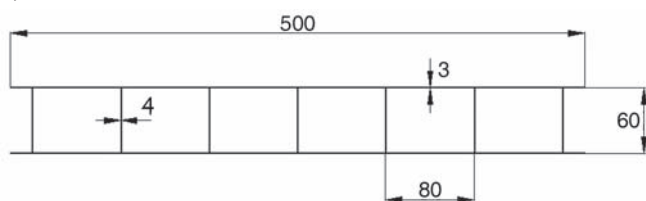
**Keywords :** laser-welded steel panels, ultimate strength of steel structures, finite element method calculations in the non-linear range

## INTRODUCTION

A research project concerning engineering processes and strength of steel panels was conducted at Faculty of Ocean Engineering and Ship Technology, Gdańsk University of Technology, [2]. Within the frame of the project manufacturing process of steel panels with the use of laser welding technique was elaborated, as well as some structural strength tests of the axially compressed panels under lateral load were performed. Results of the tests are presented in [3] and [4].

Construction of a typical panel is shown in Fig. 1. It consists of flat steel plates of  $t = 3.0$  mm thickness, mutually connected by means of steel webs of  $t = 4.0$  mm thickness, 60 mm depth, and 80 mm spacing. The plates are laser-welded to the webs. Such welding technique ensures weld penetration through not full thickness of webs (Fig.1). The so obtained joint constitutes a significant notch in panel's structure and determines the immediate and fatigue strength of such structures.

### a) Cross-section



### b) Joint between plating and web

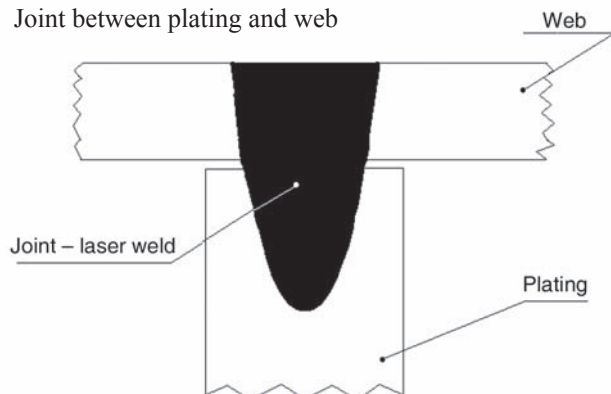


Fig. 1. Construction of the panel.

In this paper are presented results of FEM strength calculations of the axially-compressed panel of  $l = 3.0$  m in length, shown in Fig. 1a. The calculations were aimed at checking if the FEM non-linear calculations where shell model of the panel has been applied, provide values of ultimate loads of the panels under axial compression, close to those experimental, described in [3] and [4]. Possible application of the simple theory of eccentrically compressed rod, proposed in [1], to ultimate strength assessment of compressed panels, is also discussed.

## ELASTIC BUCKLING OF THE COMPRESSED PANEL

Strength of the panel under axial compression was assessed by using the model of compressed rod of the cross-section as in Fig. 1,  $l = 3.0$  m in length, and hinge-supported ends.

In this case the theoretical critical stresses  $\sigma_E$  are as follows :

$$\sigma_E = \frac{\pi^2 E I}{l^2 A} \quad (1)$$

where :

$E = 2.06 \cdot 10^5$  N/mm<sup>2</sup> - Young modulus of steel  
 $I = 3.483 \cdot 10^{-6}$  m<sup>4</sup> - inertia moment of the cross-section shown in Fig. 1a  
 $l = 3.0$  m - length of the rod  
 $A = 4.68 \cdot 10^{-3}$  m<sup>2</sup> - cross-sectional area of the rod shown in Fig. 1a.

From the calculations by using (1) the following was obtained :  $\sigma_E = 168$  MPa.

The value of the theoretical critical force  $P_E = \sigma_E A = 0.786$  MN.

The elastic buckling of the panel under axial load was investigated also by using FEM calculations with application of NEi/Nastran computer software [5]. The applied FEM model is shown in Fig. 2.

The model was built of the quadrilateral four-node finite shell elements of CQUADR type placed in the mid-thickness of panel plating. In such model the details of the plate-web joints shown in Fig. 1b, are not taken into account. The linear elastic

stress-strain model of the material having Young's modulus  $E = 2.06 \cdot 10^5$  MPa and Poisson's ratio  $\nu = 0.3$ , was assumed.

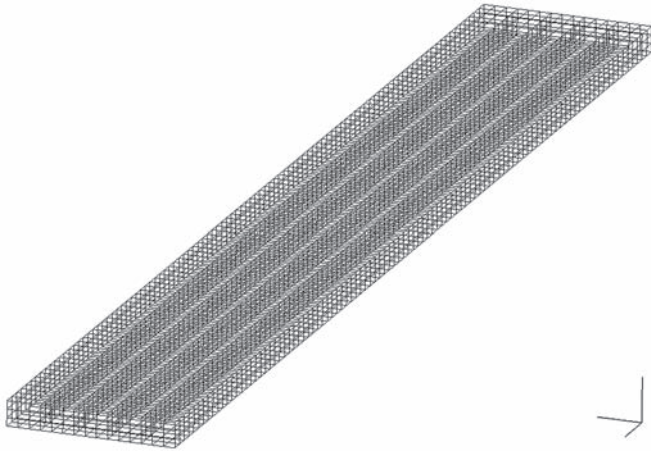


Fig. 2. The FEM model of the panel, used for elastic buckling calculations .

The calculated value of the theoretical critical force (total compression force applied to the panel) relevant to the basic form of elastic buckling shown in Fig.3, amounts to  $P_E' = 0.800$  MN. The force  $P_E'$  is greater only by 1.8% than  $P_E$ . It is consistent with expectations that  $P_E' > P_E$ . As a rule FEM model yields an excessively large value of structural stiffness.

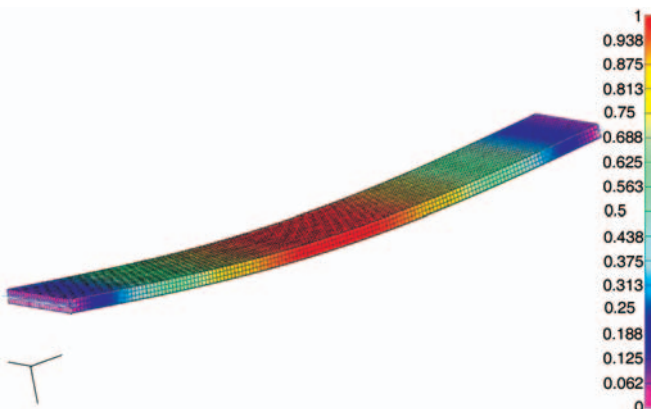


Fig. 3. The basic form of elastic buckling .

### ULTIMATE STRENGTH CALCULATIONS OF COMPRESSED PANEL

In the FEM calculations, plastic flow of material and influence of deformations (panel deflections) on values of internal forces and stresses were taken into account. The material plastic flow was assumed in compliance with the model based on associate principle of plastic flow. The assumed simplified  $\sigma - \epsilon$  characteristics of material under uniaxial tension/compression is shown in Fig.4.

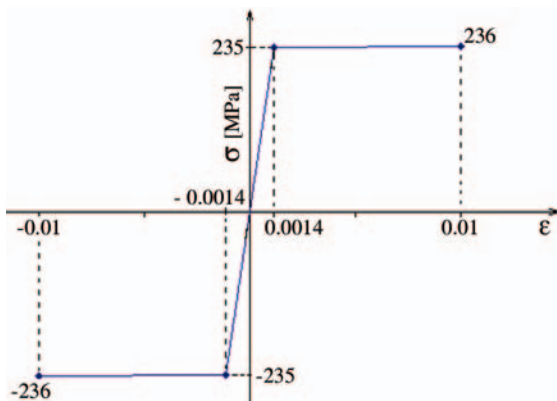


Fig. 4. The assumed  $\sigma - \epsilon$  characteristics of material .

It was assumed that the panel is freely-supported at the ends, and some longitudinal displacements of one of the ends were uniformly exerted to all webs (the support and forced displacements were applied to the points at the mid-depth of the webs). The FEM model of the panel, built of quadrilateral finite shell elements of CQUADR type (acc. [5]) is presented in Fig.5. The model does not take precisely into account the features of the welded joint connecting web and plating, shown in Fig.1b.

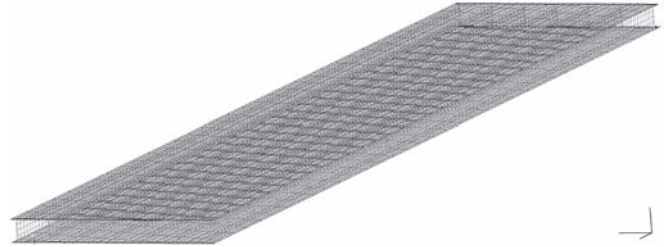


Fig. 5. FEM model of the panel .

The calculations were performed for the panel with an imperfection assumed in the form of an initial cylindrical deflection in the plane of the webs. The shape of the initial deflection was approximated with the use of third-order spline (of zero-value of second derivatives at ends), symmetrically with respect to the plane perpendicular to the webs, at their mid-length. The calculations were performed for a few values of the initial deflection  $\delta$ , namely: 2.5 mm, 5.0 mm, 7.5 mm and 10 mm.

The NEi/Nastran software was used again. The calculations consisted in determining the state of equilibrium of the panel, corresponding with successive, systematically increasing values (steps) of the longitudinal displacement of one of the panel's ends,  $\Delta l$ . The assumed step of set displacements was equal to 0.5 mm.

The typical damage mode of the structure is shown in Fig.6 (initial deflection of 2.5 mm ;  $\Delta l_{max} = 12.5$  mm)

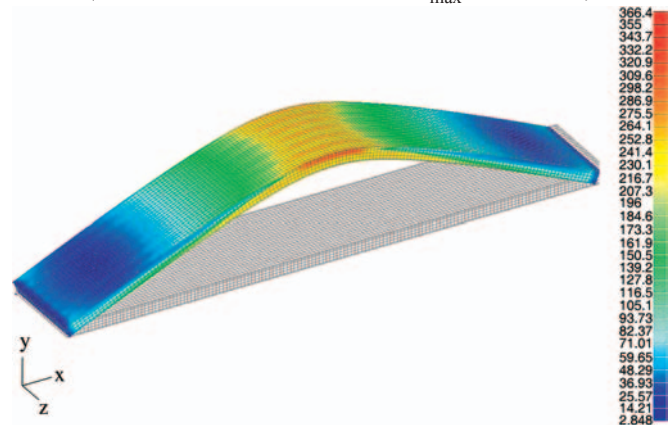


Fig. 6. Mode of the panel's damage .

In the diagrams in Fig.7 is shown the value of the compressive force  $P$  applied to the panel in function of the decrease of distance between its ends, obtained from solving the above described non-linear FEM model.

The maximum values  $P_{max}$  of  $P$  forces in the diagrams (Fig.7) are considered as the critical forces (ultimate strength) of the axially compressed panels. They are presented in Table.

In Table are also presented values of the critical forces estimated with the use of the theory described in [1]. The theory concerns the axially compressed rod with initial deflection of the maximum value  $\delta$  at its mid-length.

As defined by this theory, the ultimate strength of the rod is deemed exhausted when the extreme value of summary stresses



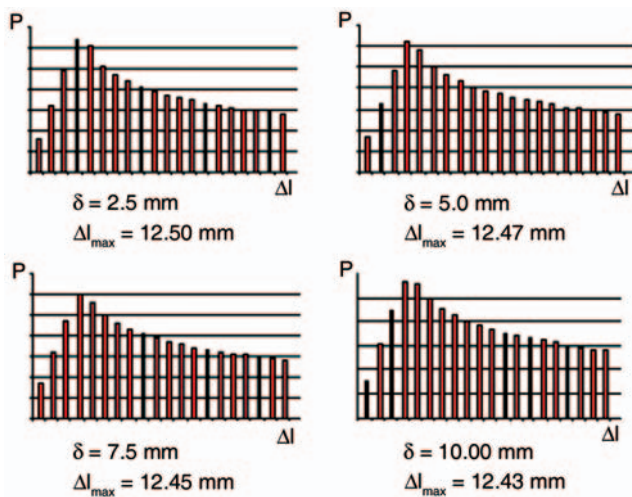


Fig. 7. The value of the compressive force  $P$  applied to the panel versus the decrease of distance between its ends.

in extreme fibres of the rod, resulting from axial compression and bending due to initial deflection of the rod, exceeds the level of yield strength of material. If to assume that the compressive force is applied just to the rod's axis and the rod is freely-supported at its both ends then the above mentioned condition can be described by the following equation :

$$\sigma_Y = \frac{P_u}{A} + \frac{P_u \delta}{\left(1 - \frac{P_u}{P_E}\right) Z} \quad (2)$$

where :

$\sigma_Y$  - yield strength

$P_u$  - extreme value of compressive force

$A$  - cross-sectional area of the rod

$\delta$  - maximum value of initial deflection

$Z$  - strength modulus of cross-section of the rod

$P_E = \frac{\pi^2 EI}{l^2}$  - theoretical value of the critical force

$E$  - Young modulus

$I$  - inertia moment of cross-section of the rod

$l$  - length of the rod.

In the equation (2) were applied : the parameters  $A$ ,  $Z$ ,  $I$  of the cross-section shown in Fig. 1a, the panel's length  $l = 3.0$  m, as well as the properties of normal steel ( $E = 2.06 \cdot 10^5$  MPa,  $\sigma_Y = 235$  MPa). On this basis  $P_u$  values were determined for a few values of  $\delta$ , as presented in Table.

Table. Critical values of the compressive force applied to the panel.

| $\delta$<br>[ mm ] | $P_{max}$ - from FEM<br>calculations<br>[ MN ] | $P_u$<br>- acc. Eq. (2)<br>[ MN ] |
|--------------------|--|-----------------------------------|
| 2.5                | 0.646  | 0.657                             |
| 5.0                | 0.624  | 0.587                             |
| 7.5                | 0.600  | 0.537                             |
| 10                 | 0.567  | 0.500                             |

As can be observed, an almost ideal conformance between the values of  $P_{max}$  and  $P_u$  acc. Hughes theory, occurs for  $\delta = 2.5$  mm. Along with  $\delta$  increasing,  $P_u$  values become increasingly smaller than  $P_{max}$  value; the difference reaches 12% for  $\delta = 10$  mm. The Hughes theory provides conservative results useful for initial estimation of ultimate strength of the panels having the structure shown in Fig.1.

And, the  $P_u$  value experimentally determined for the panel with the initial deflection of  $\sim 7.0$  mm amounts to about 0.77 MN, [3] and exceeds the value  $P_{max}$  for  $\delta = 7.5$  mm (0.600 MN) (from Table) by about 25%. The difference can be explained by the fact that the real value of yield strength of the material is greater than  $\sigma_Y = 235$  MPa assumed for FEM calculations. Even if the yield strength is exceeded the applied steel is capable of transferring much greater stresses than those resulting from the  $\sigma - \epsilon$  relationship assumed for FEM calculations (Fig.4).

In the experiment appears also some constraints against rotation around the transverse axis of the end cross-sections of the panel whereas in the FEM model the hinge support of the panel ends was assumed.

The forces  $P_{max}$  presented in Table are considerably smaller than the above given value of the theoretical force  $P_E = 0.800$  MN.

## FINAL CONCLUSIONS

The FEM calculations and those performed by using the simple theory of rod longitudinal bending, proposed in [1], show that the influence of initial deflections of the panel on ultimate values of compressive force, is considerable (Table). The ultimate force values decrease along with the maximum initial deflection increasing. Simultaneously, the forces calculated in compliance with [1] are smaller than those calculated by using the FEM (except of the case of a small value of initial deflection, namely  $\delta = 2.5$  mm) and the difference increases along with the maximum initial deflection  $\delta$  increasing, and it reaches about 12% for  $\delta = 10$  mm. Hence the simple theory acc. [1] is applicable for conservative estimation of ultimate strength of axially compressed panels.

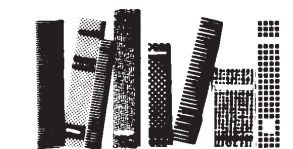
It is characteristic that the time-consuming, non-linear calculations by using the FEM model also provide the conservative results even greater by about 25% as compared with the experimental ones. This can be explained by the fact that the  $\sigma - \epsilon$  relationship of lowered values of  $\sigma$  was applied for the calculations, as well as by different conditions in supporting the panel's ends, those assumed for the FEM model and those really existing during the experimental tests.

## NOMENCLATURE

- $t$  - plate thickness
- $\epsilon$  - unit strain
- $\nu$  - Poisson's ratio

## BIBLIOGRAPHY

1. Hughes Owen F. : *Ship Structural Design – A Rationally Based Computer Aided Optimisation Approach*, The Society of Naval Architects and Marine Engineers, 1988
2. Kozak J.: *Steel sandwich panels – novel structural elements for ships* (in Polish). Proc. of the 20th Scientific Session of Naval Architects and Marine Engineers. Gdańsk 2002
3. Kozak J.: *Strength tests of steel sandwich panels. Maritime Transportation and Exploitation of Ocean and Coastal Resources*. Proc. of the 12th Int. Congress of the Int. Association of the Mediterranean (IMAM 2005), Lisboa 26-30 Sept. 2005. Taylor&Francis
4. Kozak J.: *Strength tests of steel sandwich panels.*, Proc. of the International Conference on Innovative Materials and Technologies of Surface Transport (INMAT 2005). Gdańsk 7-8 Nov.2005.
5. NEI/Nastran Reference Manual, ver. 8.4. Noran Engineering Inc., 2005



# FEM strength analysis of sandwich panels for ship structure applications

Marek Augustyniak, M.Sc., Eng. }  
Grzegorz Porembski, M.Sc., Eng. } DESART Company Ltd.

## ABSTRACT

*This paper presents results of the numerical simulation modelling strength tests of laser-welded, foam-filled steel panels, performed by means of the Finite Element Method (FEM) within the frame of the ASPIS project. In this case application of the FEM makes it possible to significantly lower costs of determination of mechanical properties and optimization of the structure respective to its strength-weight ratio. The entire project as well as the presented calculations are aimed at implementing structures of the kind to shipbuilding industry. Results of the calculations modelling axial compression of panels comply with experiments qualitatively. The entire process of the structure's compression till its collapse resulting from extensive plastic deformation within its middle zone, was step-by-step examined. Also, critical forces causing instability of the structure were determined. A partial quantitative discrepancy of the calculated reaction forces and those experimentally measured, requires further investigations.*

**Keywords** : sandwich structures, plastic buckling, Finite Element Method (FEM)

## INTRODUCTION

Sandwich panel structures (SPS) are more and more widely applied in various industrial branches, a.o. in building [1,2] and aircraft industry. Their high density/strength ratio makes them an attractive alternative for traditional ship structures. A part of the solutions has been already standardized [3], however the SPS are continuously optimised in the world.

At Gdańsk University of Technology in the frame of ASPIS project were performed laboratory tests of large-scale prototypes of steel panels to be applied – after their optimisation – to ship hulls. Implementation of such structures requires first of all to determine their resistance to tension and bending loads, as well as to design optimum joining systems and optimise their strength/mass ratio and cost. Because of large costs of experimental tests it was decided to conduct a part of the investigations by means of the finite element method (FEM) [4].

In this paper are presented results of numerical simulations of behaviour of such panels under uniaxial compression along axis of stiffeners (webs) where influence of two parameters : laser-weld width and web depth, has been considered. Five variants of weld width (1, 1.5, 2, 3 and 4 mm) and two variants of web depth (20 and 60 mm) were assumed in accordance with the series of types established by the project co-ordinators. *I-core* panels filled with polyurethane foam, were built of 3 mm steel shell plating and 4 mm webs of 80 mm depth. The overall dimensions of a single panel reached 6000x1000 mm.

The calculations in question were performed with the use of two methods. Results from the first of them was assumed to be the first approximation. It consisted in determining the critical buckling force for the panel, the other – in step-by-step investigating the course of the compression process of the structure till its collapse resulting from extensive plastic deformations in its middle zone. The instant of collapse was arbitrary assessed – it was assumed that the occurrence of visible local buckling of cover plates in the plane of the maximum deflection of the panel stands for the state of sandwich panel collapse.

## FEM MODEL

In accordance with the real prototype structure the higher strength steel RAEX 355 MC LASER (of the tensile strength  $R_m = 450 - 510$  MPa, and the yield strength  $R_e = 355$  MPa) was selected for shell plating (cover plates) and St3 structural

steel (of  $R_m = 425$  MPa, and  $R_e = 235$  MPa) for webs. As  $R_m$  value of the first steel was given within certain range, for the calculations its mean value equal to 480 MPa was assumed. Both the steels were characterized by the same initial value of Young modulus equal to 206000 MPa. The bilinear strain-stress model was assumed in which elastic behaviour is valid within small deformation range only and beyond it the material behaves in compliance with the following hardening modulus formula :

$$E_{tt} = (R_m - R_e) / [(A5 / 100) + (R_m - R_e) / EX]$$

where :

- $R_m$  – tensile strength
- $R_e$  – yield strength
- A5 – total elongation of the A5 specimen after breaking
- EX – Young modulus

Copper material of the distance plate between the steel pad to which the compressive load is applied, and the tested panel itself, is characterized by the single Young modulus equal to 100000 MPa. For the polyurethane foam filling the Young modulus of 12 MPa was assumed.

The FEM model consisted of about 13.000 SOLID186 finite elements as well as CONTA174 and TARGE170 contact ones placed in the gap in the laser-weld area.

The panel underwent full parametrisation process, and its most important parameters were in accordance with the authors' notation, as follows :

- DC - internal distance between cover plates
- DIVDC - number of divisions over the web depth
- L1 - web thickness
- T1 - plating thickness
- SC - gap between plating and face of web end
- SP - weld width
- RX - web spacing
- PPZ - area to be analysed along web axis
- PODZZ - division into elements in the indicated direction
- APODZZ - concentration of the division into elements in the indicated direction
- ILP = 6 - number of closed boxes
- PPX - area to be analysed in the direction perpendicular to webs



On the basis of several test computations it was determined that the minimum number of divisions along webs of the panel 3000 mm long, was equal to 10, hence for the main analyses 14 divisions gradually denser towards the plane of maximum deflection of the panel, were assumed.

**RESULTS**

Table shows the critical force values determined from the linear buckling analysis, at which the panel buckling and collapse takes place.

Values of maximum reaction forces [N].

| Weld width [mm] | Model No. 3 (web of 20 mm depth) | Model No. 12 (web of 20 mm depth) |
|-----------------|----------------------------------|-----------------------------------|
| 1.0             | 89112                            | 382778                            |
| 1.5             | 89240                            | 382254                            |
| 2.0             | 89315                            | 382778                            |
| 3.0             | 89414                            | 383299                            |
| 4.0             | 89462                            | 383592                            |

The below presented diagrams show values of the reaction force recorded during gradual shifting the compression machine traverse, with the step of 1 cm. The results were obtained from the non-linear elastic-plastic analysis.

Weld width of 2 mm, Model No.3 (20 mm web depth)

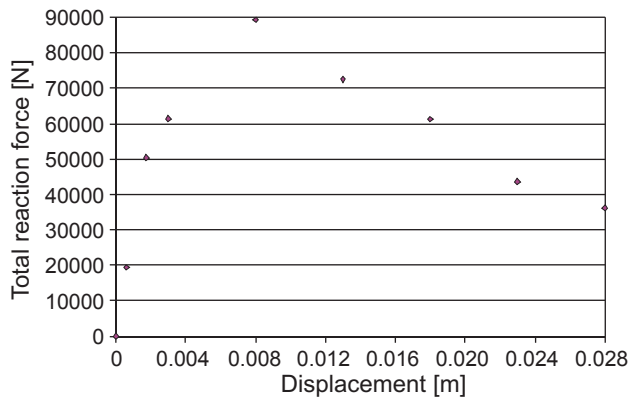


Fig.1. Reaction force values obtained from elastic-plastic analysis.

Weld width of 2 mm, Model No.12 (60 mm web depth)

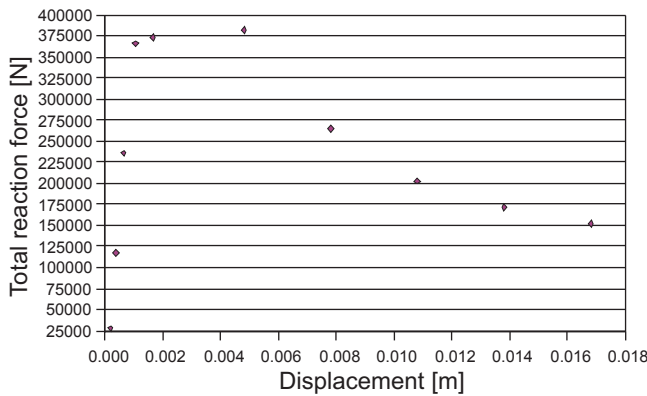


Fig.2. Reaction force values obtained from elastic-plastic analysis.

Some contour maps are attached in the end of this paper. Fig.5 and 6 show deformations in the middle plane of the panel model of 1 mm weld width and 20 mm or 60 mm web depth, respectively. Fig.7 and 8 illustrate the reduced stresses in the

panel model of 20 or 60 mm web depth, respectively. Fig.9 and 10 present results for another variant of the panel, namely that of 60 mm web depth and 3 mm weld width, where the plastic deformations and reduced stresses compared with those for the panel model of 1 mm weld width, as an example, can be found.

Important seems to be a comparison of the results of the linear-buckling analysis and elastic-plastic one. The first yields the critical force value of about 94 kN and 780 kN, for 20 mm and 60 mm web depth, respectively. The increase of the critical force value by almost one order of magnitude as a result of tripling the web depth, complies with the Euler theory of plates (the critical force increase proportional to the square of plate thickness).

The observed very small influence of weld width on the critical force is hard to be explained. However it can be argued that the joints between cover plates and webs do not transfer any significant loads under compression, and the FEM analysis shows that in the vicinity of the welds are present no significant stresses which could trigger a failure mechanism dependent in a certain way on width of the welds.

The full non-linear analysis with plastic deformations taken into account brings – for 20 mm web depth – the results identical with those from the linear analysis. In the case of 60 mm web depth an excessively sparse step of calculations was assumed that resulted in omitting a peak value of reaction force. However the run of the functions on both sides of the critical range of deformations indicates that also for 60 mm depth of webs the critical force could achieve a value close to that calculated from the linear-buckling analysis. The assumed sparse step of calculations was forced by hardware and time limitations.

The form of local failures of the panel is worth observing (Fig.3 and 4). In the plane of the maximum deflection of the panel after global buckling, reaching more than 20 cm, also

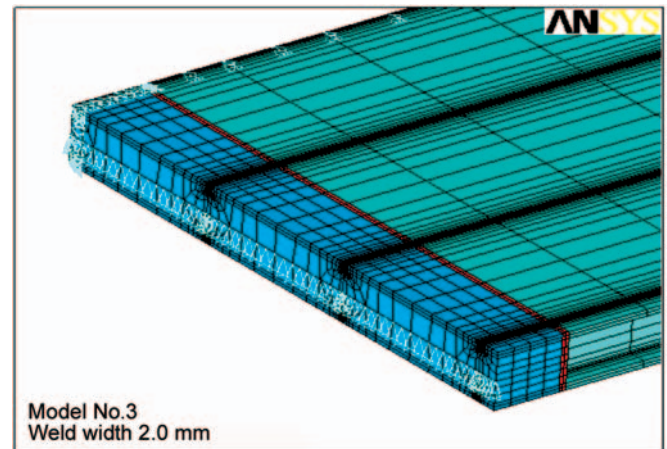


Fig. 3. A view of compression traverse.

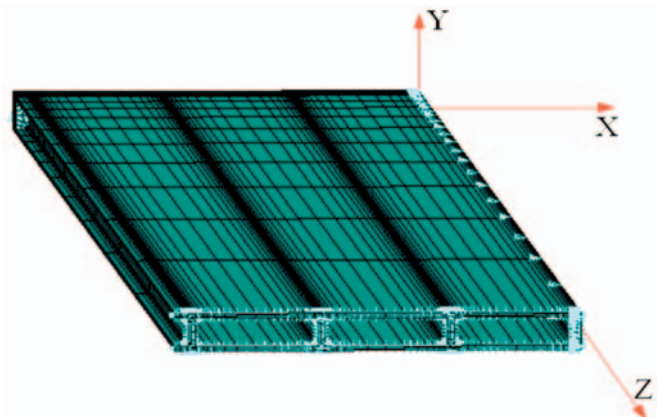


Fig. 4. A quarter of FEM model with supports.

local buckles of cover plate strips between neighbouring webs, occur. The alternating sense of the maximum local deflections of the plates which underwent buckling, is characteristic.

At the end, worth mentioning is the correct qualitative conformity and quantitative discrepancy of the experimental and numerical simulation results. Reasons for the discrepancy could be associated with an insufficient density of numerical model mesh along the webs, which constitutes a compromise between calculation accuracy and hardware capabilities and cost of the research. Another possible cause can be some discrepancy between the way of modelling of the copper distance plate and the traverse compressing the panel.

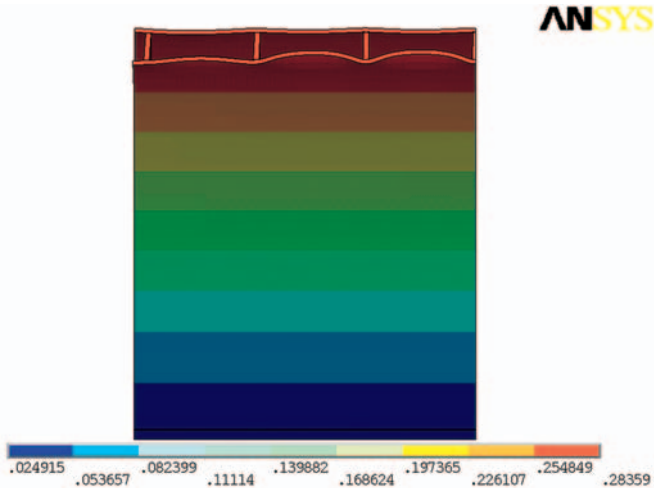


Fig. 5. Displacements and failure mode of the panel of 20 mm web depth and 1 mm weld .

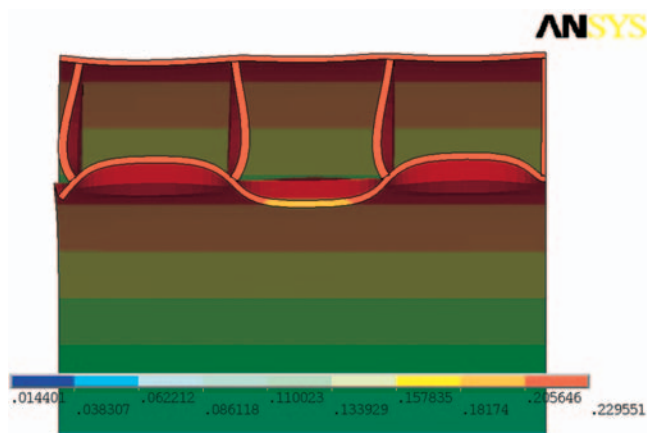


Fig. 6. Displacements and failure mode of the panel of 60 mm web depth and 1 mm weld .

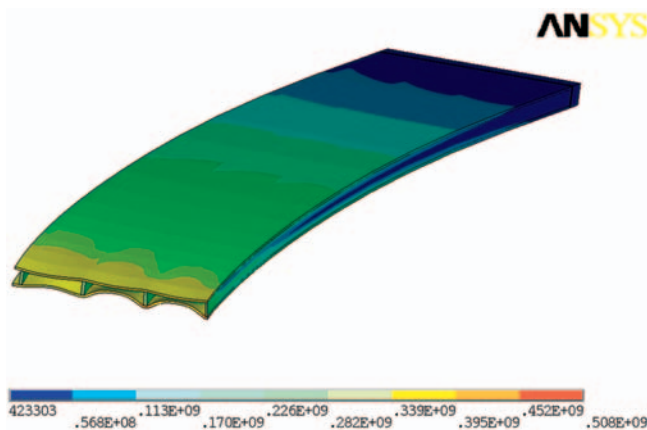


Fig. 7. Reduced stresses in the panel of 20 mm web depth and 1 mm weld .

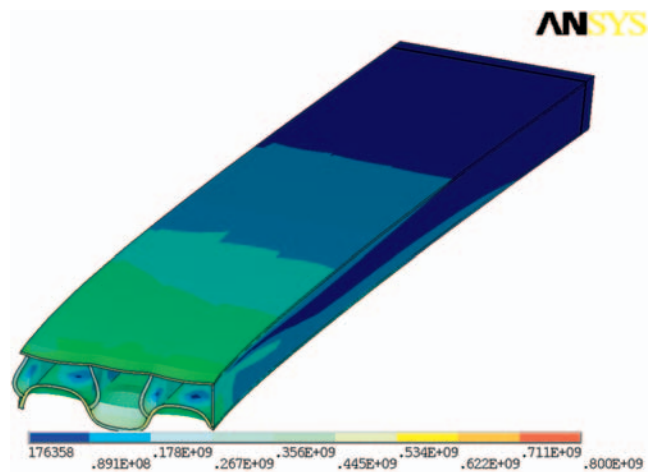


Fig. 8. Reduced stresses in the panel of 60 mm web depth and 1 mm weld .

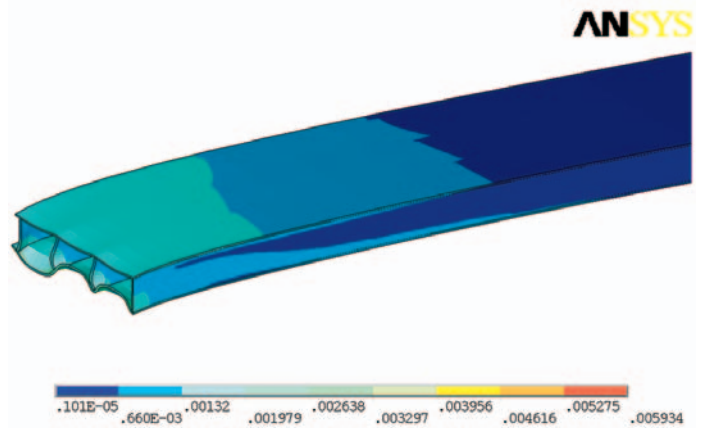


Fig. 9. An example map of plastic deformations in the panel of 60 mm web depth and 3 mm weld .

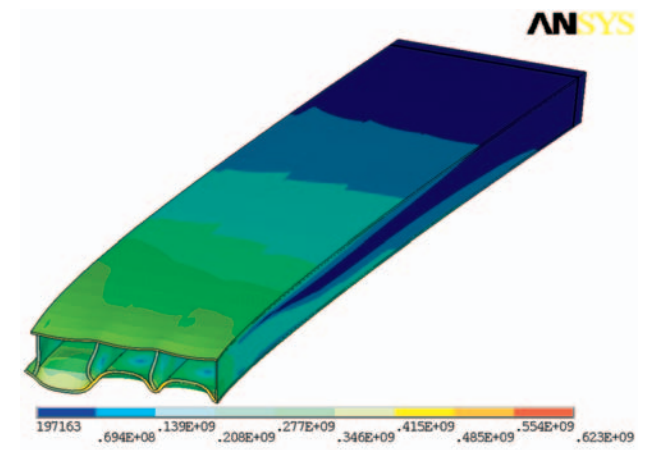


Fig. 10. Reduced stresses in the panel of 60 mm web depth and 3 mm weld .

#### BIBLIOGRAPHY

1. Brown D., Kennedy S.J., Kennedy D.J.L., Allen D.E.: *Sandwich Plate System Risers for Stadia*, SSRC 2002 Annual Stability Conference, Seattle, Washington, 24-27 April 2002
2. Vincent R. B., Ferro A.: *Design and construction of the Shenley bridge incorporating an SPS orthotropic bridge deck*. Orthotropic Bridge Conference, Sacramento, USA, August 2004
3. Lloyd's Register : *Provisional rules for the application of sandwich panel constructio to ship structure*, April 2006
4. Augustyniak M., Porembski G.: *FEM analysis of a single sandwich panel compressed along its strengthening elements* (in Polish). Report on the calculations performed within the ASPIS project (in Polish). Internal materials of the DESART Co. Gdańsk, 2005



# Fatigue life tests of steel laser-welded sandwich structures

Dariusz Boroński,  
Józef Szala  
University of Technology  
and Agriculture, Bydgoszcz

## ABSTRACT

*This paper presents results of the fatigue life tests of elements of steel laser-welded sandwich structure, performed at the Department of Machine Design, University of Technology and Agriculture, Bydgoszcz, in cooperation with the Department of Ship and Offshore Structures Technology, Gdańsk University of Technology, within the frame of ASPIS EUREKA E13074 project titled : „Application of steel sandwich panels into ship structural design”. The obtained information on fatigue features of various specimens, the so called elementary structures of sandwich panels, can make it possible to formulate design and manufacturing recommendations for application of such structures in shipbuilding. An important result of the performed tests is the extended range of fatigue strength data for laser-welded joints.*

**Keywords:** fatigue; laser welding; fatigue life diagrams; steel panel structures

## INTRODUCTION

Application of welded joints to building large objects intended for working under changeable loads requires taking into account hazards associated with initiation and propagation of fatigue cracks. Regardless of used fatigue life analysis methods [1] the condition of effectiveness of conducted calculations is to have knowledge on fatigue features of applied welded joints. It is specially important in the case of implementation of novel welding techniques such as laser welding, for which sufficient fatigue data are still lacking.

According to literature sources, there is a lack of commonly applicable guidelines for fatigue life analysis of laser-welded joints, which is the case of traditionally manufactured welded joints [2]. Moreover, the existing results of high-cycle (elastic strain) fatigue tests of smooth specimens containing laser-welded joint [3] indicate that their fatigue strength is close to that of native material.

The problems clearly concern also laser-welded sandwich panel structures constituting the subject of the tests realized within the frame of the ASPIS EUREKA E13074 project titled : „Application of steel sandwich panels into ship structural design”.

Assessment of fatigue features of such structures constituted one of the aims of the tests carried out at the Department of Machine Design (PKM), University of Technology and Agriculture, Bydgoszcz, in cooperation with the Department of Ship and Offshore Structures Technology, Gdańsk University of Technology, which took part in realization of the ASPIS project.

The tests were carried out at the PKM Laboratory accredited by the PCA (Polish Centre of Accreditation).

## PROGRAM AND OBJECTS OF THE TESTS

The program of the tests of elements of steel panel structure has been presented in the form of the block diagram shown in Fig.1. It contains three groups of tests :

- tests under monotonous loading
- preliminary fatigue tests
- main fatigue tests.

The basic aim of the monotonous tests was to determine main static properties of the material specimens as well as elementary structures of various forms. On this basis preliminary ranges of loads used in the fatigue tests were determined among other. Within the frame of the preliminary tests geometrical features of the specimens were verified and finally selected, as well as – in view of complexity of stress and strain distributions in joint – load conditions for the main tests were determined.

Tests of the strain distributions distinguished by broken line in Fig.1, covering the analysis of local

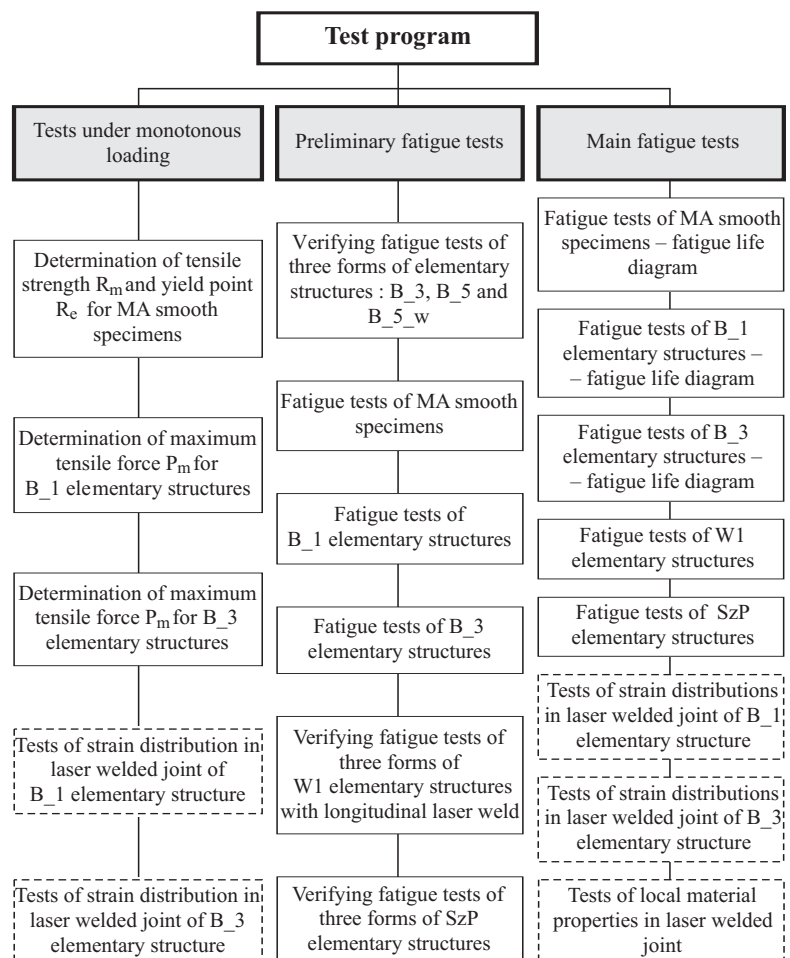


Fig.1. Schematic diagram of test program .

strain distributions in laser-welded joints of various elementary structures, constituted a separate scope of the investigations. Some part of the results of the tests were discussed in [4].

The elementary structures used in the tests represented various cases of weld location respective to load direction. Dimensions and geometrical forms of the specimens taken from a steel sandwich panel are shown in Fig.2 and 3.

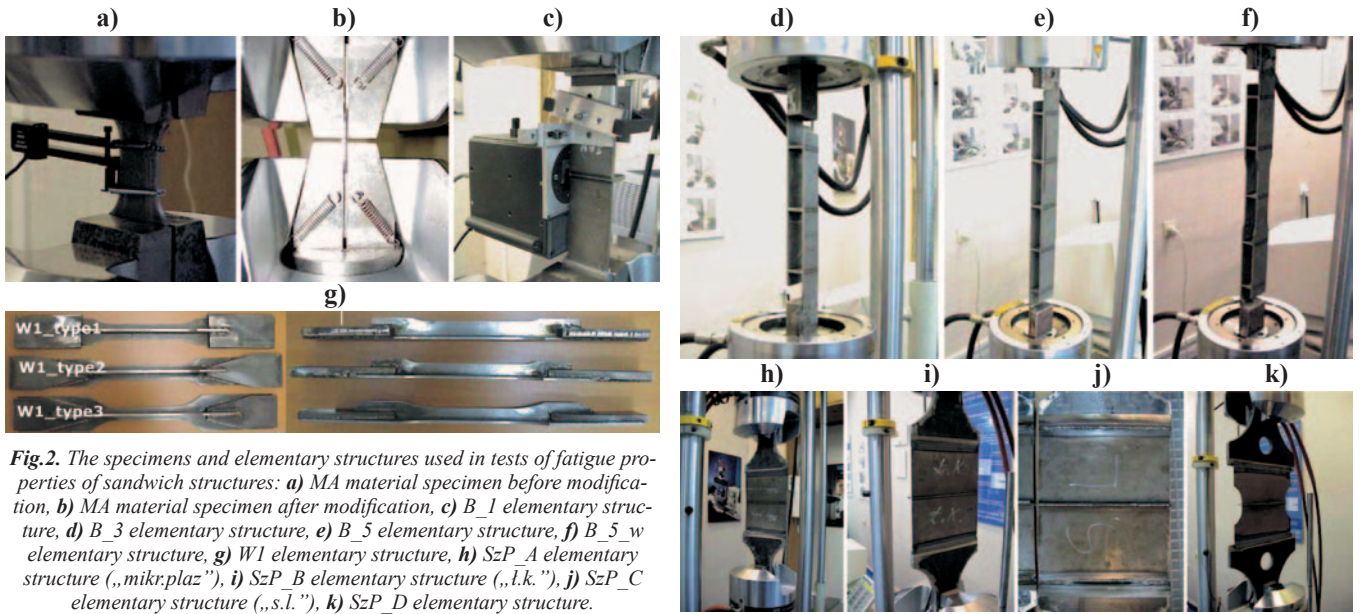


Fig.2. The specimens and elementary structures used in tests of fatigue properties of sandwich structures: a) MA material specimen before modification, b) MA material specimen after modification, c) B\_1 elementary structure, d) B\_3 elementary structure, e) B\_5 elementary structure, f) B\_5\_w elementary structure, g) W1 elementary structure, h) SzP\_A elementary structure („mikr.plaz”), i) SzP\_B elementary structure („l.k.”), j) SzP\_C elementary structure („s.l.”), k) SzP\_D elementary structure.

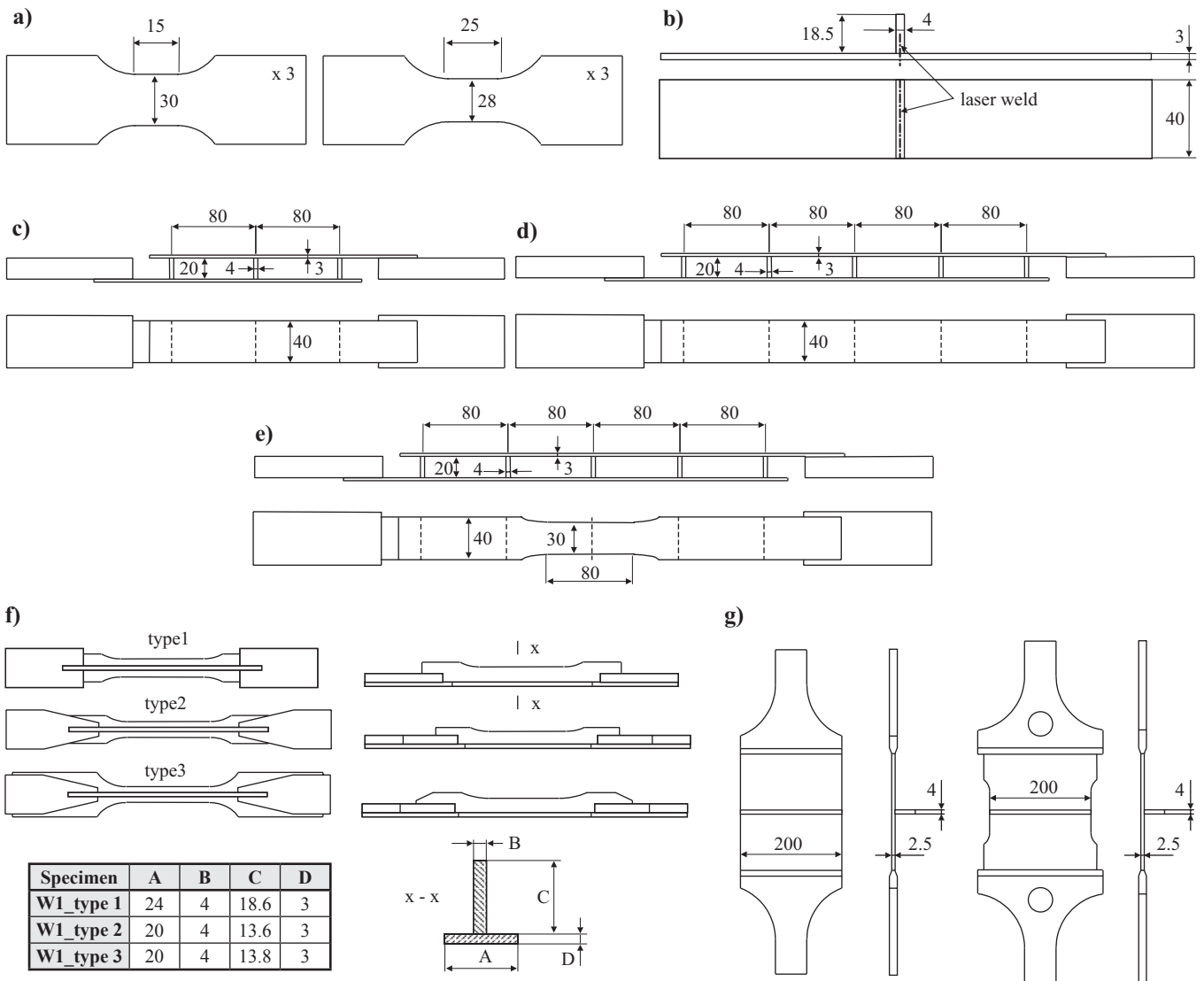


Fig. 3. Nominal main dimensions of elementary structures of sandwich panel: a) MA material specimen before and after modification, respectively, b) B\_1 elementary structure, c) B\_3 elementary structure, d) B\_5 elementary structure, e) B\_5\_w elementary structure, f) W1 elementary structures : type 1, type 2 and type 3, g) SzP elementary structure.



The tests of smooth specimens and elementary structures were performed according to the PCA procedures approved in the AB372 certificate, in compliance with the PN-EN 10002-1+AC 1:1998 standard – in the case of monotonous loading, and the PN-74/H-04327 standard – in the case of fatigue loading. The fatigue tests were performed in the conditions of controlled variability of force.

### RESULTS OF THE TESTS

The detail description of results of the tests carried out in accordance with the particular points of the assumed program, is contained in the reports from realization of the work in the years 2003-2006 [5-8]. In this paper – because of its limited volume – are presented only the results of the main tests, given in the form of fatigue life diagrams for particular types of joints. For MA material specimens, their mechanical properties determined during monotonous tensile tests, are presented additionally.

#### MA specimens

The aim of the tests of the MA specimens was to determine static and cyclic properties of the material used for sandwich structure plating.

In Fig.4 is shown the monotonous tension diagram obtained for MA specimens, in which are marked the stress values corresponding with their plastic flow, ( $\sigma_e$ ), as well as the maximum stress values occurred in the course of loading, ( $\sigma_m$ ).

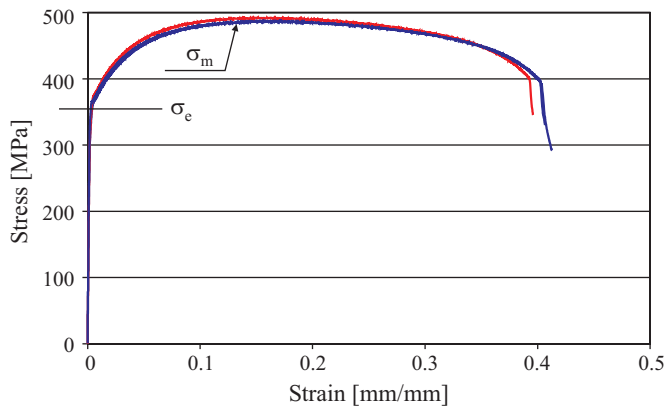


Fig.4. Diagrams of monotonous tension tests of MA specimens .

The tests of cyclic properties of the material were carried out at the controlled amplitude of the nominal stress  $S_a$ , the constant stress ratio  $R = -1$  (the mean nominal stress  $S_m = 0$ ), and the load frequency  $f = 5$  Hz. The this way obtained fatigue life diagram expressed in stresses is shown in Fig.5.

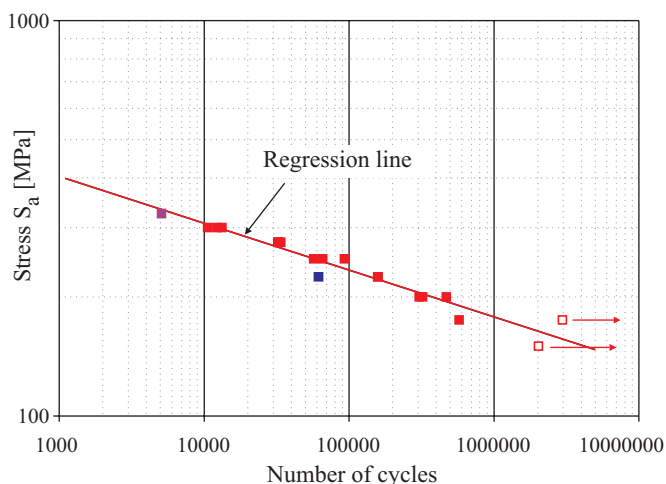


Fig. 5. Fatigue life diagram of MA specimens .

#### B-1 elementary structures

In Fig.6 is presented the fatigue life diagram obtained from the tests of B\_1 specimens. The tests were performed at the controlled force and the constant stress ratio  $R = 0$ . The data are presented in the bi-logarithmic coordinate frame. The results of fatigue life tests (of all specimens) were approximated by means of the straight line “1”. As the data on fatigue life of the specimens at the loading levels  $P = 24, 27$  and  $30$  kN were incomplete the regression line „2” was added without taking into account the results of the discontinued tests (distinguished by the arrows). Moreover, the regression line “3” was determined for the set of the data not containing those of the discontinued tests and results of the tests at the loading level  $P = 54$  kN, which already entered the low-cycle range of fatigue life.

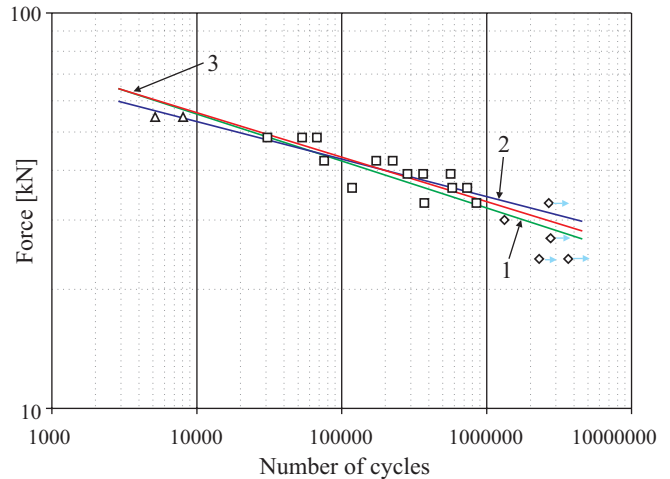


Fig. 6. Fatigue life diagrams of B\_1 elementary structures .

#### B\_3 elementary structures

Like in the case of the B\_1 specimens, tests of B\_3 specimens were carried out at the controlled force value and the constant stress ratio  $R = 0$ . As a result of the tests was elaborated the fatigue life diagram shown in Fig.7 in the bi-logarithmic coordinate frame “force – cycle number”. Results of fatigue life tests (of all specimens) were approximated by the straight line „1”. Moreover the regression line “2” for the set of data not containing those of discontinued tests, was determined.

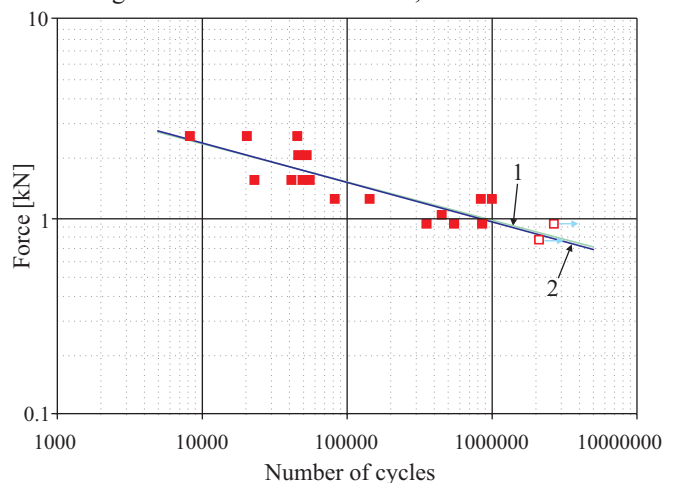


Fig. 7. Fatigue life diagrams of B\_3 elementary structures .

Analysis of the recorded runs of displacement changes made it possible to observe that the fatigue life of the specimens depended to a greater extent on the displacement range (amplitude) than on the set value of the force range (amplitude). For this reason as well as for comparison purposes was elaborated the fatigue life diagram in the coordinate frame “displacement –

– cycle number”, shown in Fig.8; this way much smaller scatter of test results was obtained. Therefore in testing such specimens the fatigue life assessment based on setting displacement amplitude is more appropriate.

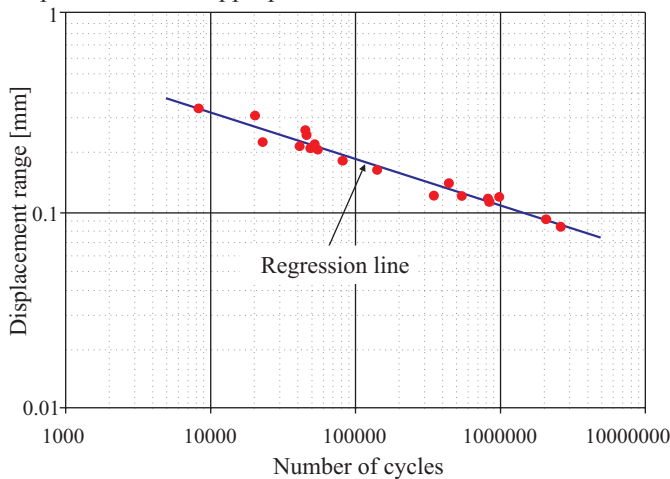


Fig. 8. Fatigue life diagram of B\_3 elementary structure, shown in the coordinate frame "displacement range – cycle number".

### W1 elementary structures

In the main tests of W1 specimens their version marked „type 3” was used. The tests were carried out at the controlled force value, the constant stress ratio  $R = 0$  and the load frequency  $f = 5$  Hz. Results of the fatigue life tests were approximated by the straight line „1” (Fig.9). Moreover the regression line “2” was determined for the set of data not containing those from two tests at the load level  $S = 425$  MPa.

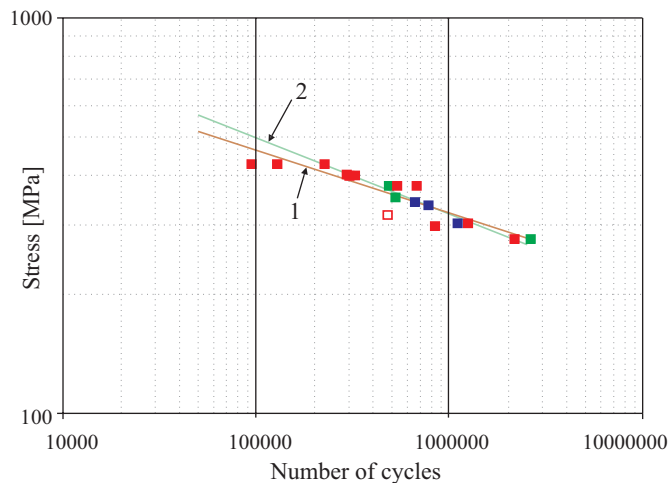


Fig. 9. Fatigue life diagram of W1\_type 3 elementary structure, shown in the bi-logarithmic coordinate frame.

### SzP elementary structures

The tests of the SzP elementary structures were carried out at the controlled force value and the constant stress ratio  $R = 0$ . In the tests the specimen version marked „SzP\_D” was used. As forms of cracks in specimens were different, to determine the fatigue life diagram shown in Fig.10 only results of the tests revealing cracks in laser weld, were selected. The results of the fatigue life tests were approximated by means of straight line.

## CHARACTERISTICS OF THE TEST RESULTS

The presented fatigue life diagrams determined by using the linear regression method were generally characterized by large values of the correlation coefficient  $R^2$ , that indicates the scatter of fatigue properties of particular specimens to be rather small.

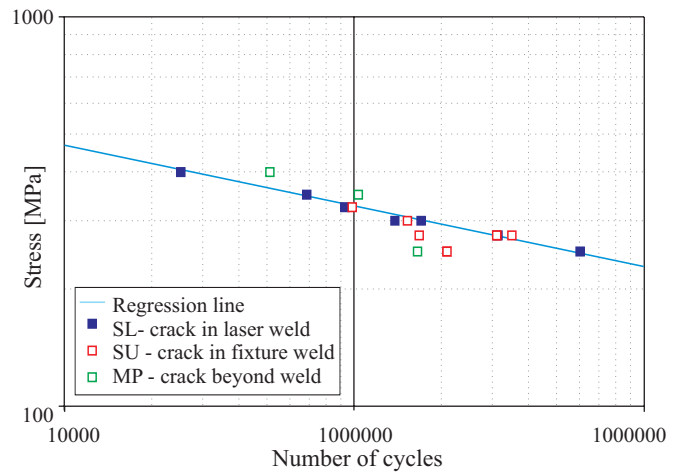


Fig. 10. Results of fatigue life tests of SzP\_D elementary structure.

It is very favourable from the point of view of the fatigue life calculation methods based on the so called design diagrams. The small fatigue life scatter of the tested specimens confirms also that laser-welded joints behave favourably, which results mainly from their high uniformity in the joint zone (repeatability of their geometrical and material features).

## SUMMARY

- The results of the performed tests constitute a rich source of data useful in analyzing fatigue phenomena occurring in steel sandwich panel structures under cyclic loading.
- The obtained information on fatigue properties of various elementary panel structures can make it possible to formulate design and manufacturing recommendations for the application of such structures to shipbuilding.
- Simultaneously, the fatigue life diagrams determined during the tests can be directly applied to fatigue life calculations of ship panel structures by using the methods based on the guidelines of Polish Register of Shipping.
- An important result of the performed tests is the extended range of fatigue strength data for laser-welded joints, indispensable in building the knowledge base on results of fatigue tests performed for structures built with the use of novel welding techniques.

## BIBLIOGRAPHY

1. Radaj D.: *Review of fatigue strength assessment of non-welded and welded structures based on local parameters*. International Journal of Fatigue 18/1996
2. Maddox S. J.: *Fatigue design rules for welded structures*. Progress in Structural Engineering and Materials, vol.2, no.1, Jan - Mar, 2000
3. Maddox S. J.: *Recommended Hot-Spot Stress Design S-N Curves for Fatigue Assessment of FPSOs*. International Journal of Offshore and Polar Engineering (Paper also given at 10th International Offshore and Polar Engineering Conference (ISOPE). Stavanger, Norway, 17-22 June 2001
4. Boroński D., Kozak, J.: *Research on deformations of laser-welded joint of a steel sandwich structure model*. Polish Maritime Research No.2/2004
5. Boroński D., Szala J.: *Fatigue tests of laser-welded specimens of sandwich structure models* (in Polish). BZ 8-2003 Report. ATR (University of Technology and Agriculture), Bydgoszcz, 2004.
6. Boroński D., Szala J.: *Fatigue tests of T- specimens with longitudinal laser weld* (in Polish). BZ 6-2004 Report. ATR, Bydgoszcz, 2004
7. Boroński D., Szala J.: *Fatigue tests of wide specimens of sandwich structure models with transverse laser weld, Phase I* (in Polish). BZ 5-2005 Report. ATR, Bydgoszcz, 2005
8. Boroński D., Szala J.: *Fatigue tests of wide specimens of sandwich structure models with transverse laser weld, Phase II* (in Polish). BZ 2-2006 Report. ATR, Bydgoszcz, 2006



# Tests of local strains in steel laser - welded sandwich structure

**Dariusz Boroński,**  
**Józef Szala**  
 University of Technology  
 and Agriculture, Bydgoszcz

## ABSTRACT

*This paper presents results of the tests of local strains in laser weld zone of steel sandwich structure, performed at the Department of Machine Design, University of Technology and Agriculture, Bydgoszcz, in cooperation with the Department of Ship and Offshore Structures Technology, Gdańsk University of Technology, within the frame of ASPIS EUREKA E!3074 project titled : „Application of steel sandwich panels into ship structural design”. Specific features of the tested structure make that in the weld zone both geometrical and structural notch appears simultaneously. The presented results may be helpful in further developing sandwich structures themselves and laser welding technique as well as their design methods as far as avoiding fatigue cracks is concerned.*

**Keywords :** fatigue, laser welding, local strain distributions, laser grating interferometry, steel panel structures

## INTRODUCTION

Fatigue life calculations of complex objects, e.g. large ship structures, can be performed with the use of many calculation methods [1,2]. Some of them are based on local approach consisting in that this is variability range of local strains and stresses in the points of their concentration, which mainly decides on fatigue life [3]. In the case of welded joints commonly used in ship structures, strain and stress concentrations are caused both by geometrical discontinuities (geometrical notches) and material non-uniformities resulting from welding process (structural notches).

An example of such simultaneous appearance of geometrical and structural notches can be the novel sandwich panel structures manufactured with the use of laser welding. Such structures constituted the subject of research realized within the frame of ASPIS EUREKA E!3074 project titled : „Application of steel sandwich panels into ship structural design”.

Experimental analysis of local strain distributions in zones of laser weld joint was one of the aims of the research carried out by the Department of Machine Design (PKM), University of Technology and Agriculture, Bydgoszcz, in cooperation with the Department of Ship and Offshore Objects Technology, Gdańsk University of Technology, a participant of the ASPIS project.

The tests were performed at the PKM Laboratory accredited by the PCA (Polish Centre of Accreditation).

## PROGRAM AND OBJECTS OF THE TESTS

The program of the tests on deformations in steel panel structure is presented in the form of the schematic diagram shown in Fig.1. It covers the tests under monotonous loading as well as those in conditions of variable loading.

The tests were performed for two types of specimens : B\_1 and B\_3 elementary structures. Main dimensions of the specimens are given in Fig.2, and places of strain measurements and loading mode of the specimens - in Fig.3. For the tests of strain distributions the laser grating interferometry technique implemented in the LES laser grating extensometer automatic system, was used. The design and working principle of the LES system was presented in detail a.o. in [4,5]. The program

of the tests of strains in steel panel structures covered also the tasks whose aim was to determine cyclic local material properties in particular laser weld zones by using the method described a.o. in [6,7]. Results of the tests within that scope will be published separately.

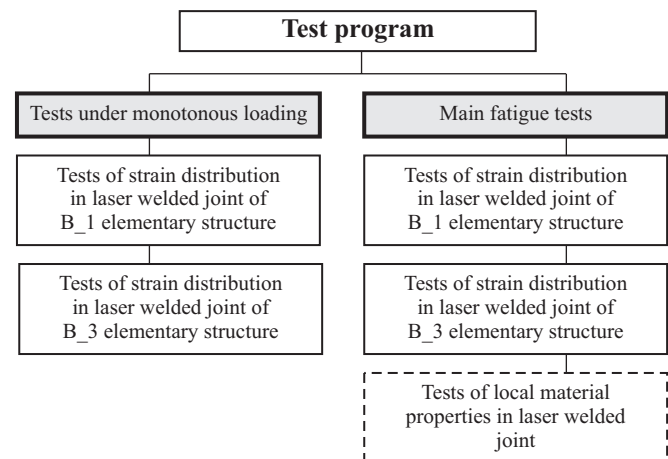


Fig. 1. Schematic diagram of test program .

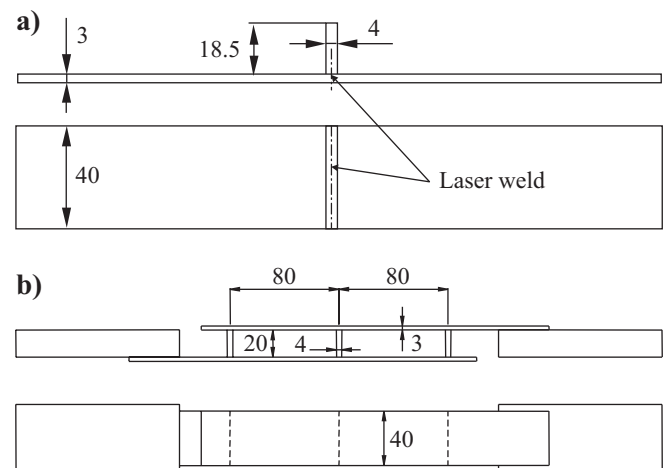


Fig. 2. Specimens, elementary structures used in strain tests :  
 a) B\_1 elementary structure, b) B\_3 elementary structure .

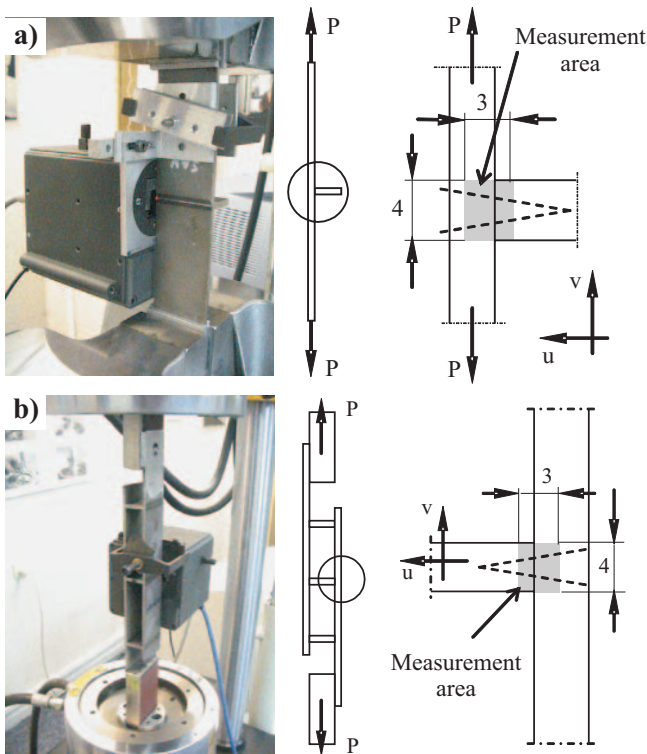


Fig. 3. Location of measurement area in :  
a) B\_1 specimen and b) B\_3 specimen .

### RESULTS OF THE TESTS AND THEIR ANALYSIS

The detail analysis of results of the tests of strains in fatigue crack zones was presented in [8]. Due to a limited volume of this paper, in its further part only example results of the measurements and conclusions drawn from their analysis, are presented. During the tests, distributions of relative displacements and strains in two mutually perpendicular directions  $v$  and  $u$  were determined on the basis of analysis of images of interference lines. In Fig.4 are shown example interferograms as well as strain distribution maps determined by means of the LES system in the course of monotonous tension test of B\_1 elementary structure.

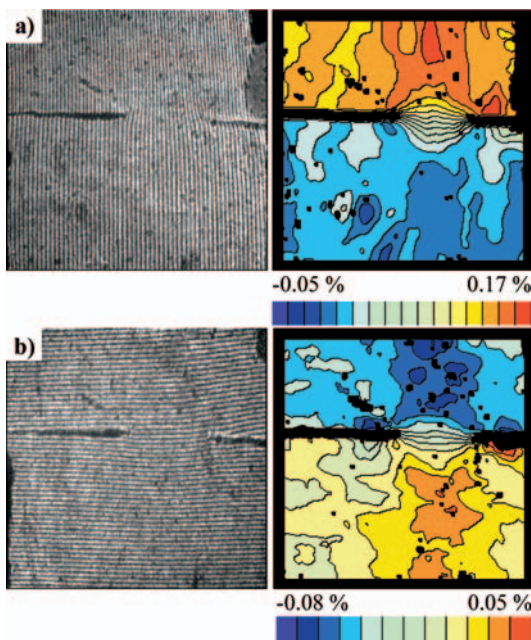


Fig. 4. Example results of measurements : B\_1 specimen, force  $P = 20$  kN,  
a)  $v$ - direction, b)  $u$ - direction .

### TESTS OF B\_1 ELEMENTARY STRUCTURE UNDER MONOTONOUS LOADING

Measurement of strains in B\_1 elementary structure under monotonous loading was performed at 49 levels of static load. The specimens were loaded in compliance with the scheme shown in Fig.3.

For particular values of the force  $P$  images of interference lines in two directions of analysis,  $v$  and  $u$ , were recorded. The measurement was carried out within  $3\text{mm} \times 4\text{mm}$  measurement area. Strain measurement places are shown in Fig.3.

In Fig.5 are shown example distributions of the strains  $\epsilon_v$  and  $\epsilon_u$ , against background of laser welded joint of B\_1 elementary structure.

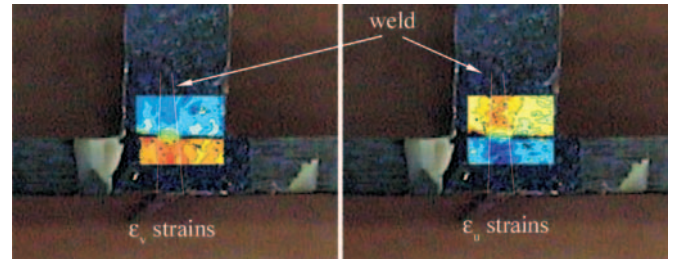


Fig. 5. Strain distributions in B\_1 specimen shown on welded joint background .

Analysis of the  $\epsilon_v$  and  $\epsilon_u$  strain distributions in selected cross-sections of the joint made it possible a.o. to observe that :

- In the analyzed area of the B\_1 structure, both in  $v$  and  $u$  strain directions, different strain values occur in the plate and web. It generates distinct strain gradients in the joint area, which can be observed in Fig. 6 and 7.

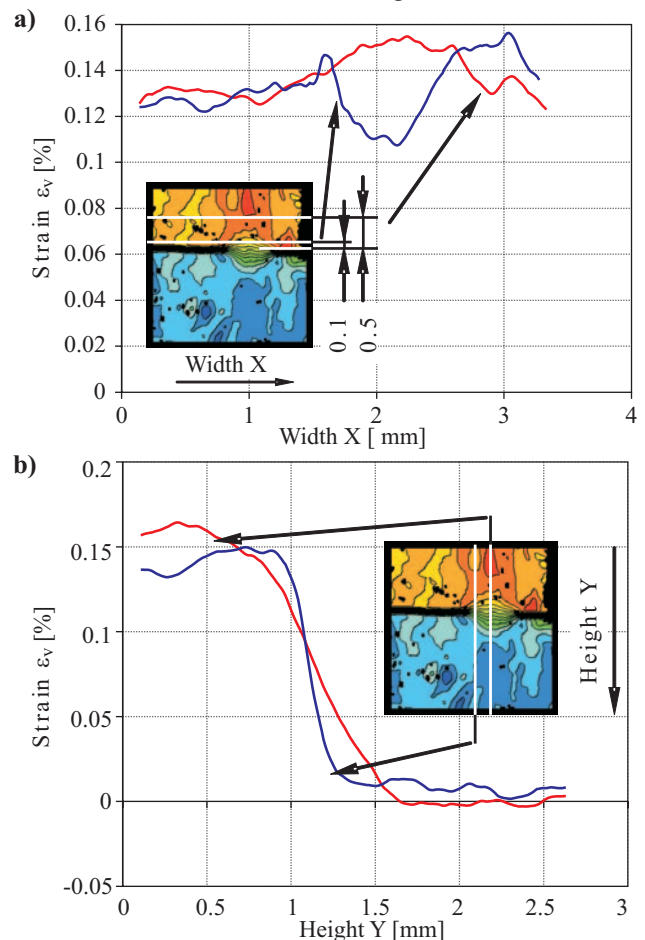


Fig. 6. ( $\epsilon_v$ ) strain distributions in B\_1 specimen in load direction : a) along specimen axis and b) transversely to it, for loading force  $P = 20$  kN .



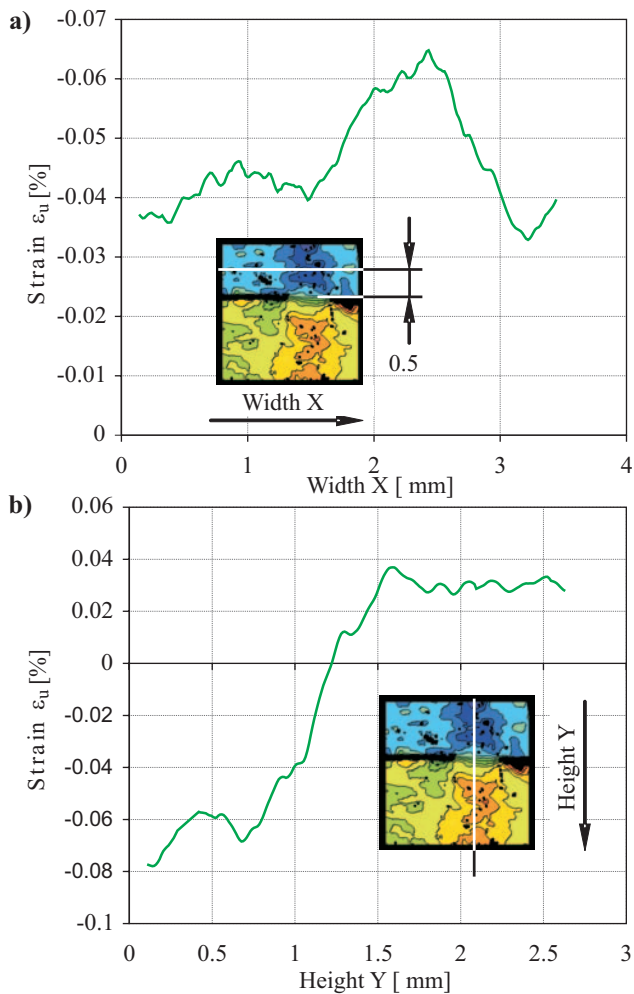


Fig. 7. ( $\epsilon_u$ ) strain distributions in B\_1 specimen transversely to load direction : a) transversely to load applied along specimen axis and b) transversely to it .

The largest difference of strain values occurs at the largest load applied to specimen and it decreases along with load decreasing.

The largest strain gradients occur in the area of transition from plate to web, at the weld edge, as well as in the transition zone between the weld and native material.

- Analysis of the strains  $\epsilon_v$  shows that tensile strains occur in the plate, and in the web the strains are close to zero. And, in the case of the strains  $\epsilon_u$  compressive strains occur in the plate, and in the web tensile strains appear in the weld zone, and beyond it strain values are close to zero similarly as in the case of the strains  $\epsilon_v$ .
- In the course of specimen loading, in the weld zone the increasing of  $\epsilon_v$  and  $\epsilon_u$  strain values occurs respective to those in native material.

### TESTS OF B\_3 ELEMENTARY STRUCTURE UNDER MONOTONOUS LOADING

In the tests of B\_3 elementary structure 16 static load levels were used. The specimens were loaded in compliance with the scheme shown in Fig.3.

Similarly as in the case of B\_1 structure, for particular values of the force P images of interference lines in two analyzed directions **v** and **u**, were recorded. The measurement was performed within 3 mm x 4 mm measurement area located in the region shown in Fig.3.

Analysis of distributions of  $\epsilon_v$  and  $\epsilon_u$  strains in laser welded joint of B\_3 elementary structure made it possible to state that :

- In the case of strains in **u**- direction, the specimen loading due to axial force, in line with the scheme of Fig.3b, generated, in the zone of the weld connecting the web with the plate, the strain gradient typical for bending load. Simultaneously the web edge exerted compression onto the outer plate, that resulted in building zones of compressive strains in the web and plate in the vicinity of the web edge. (Fig.8).

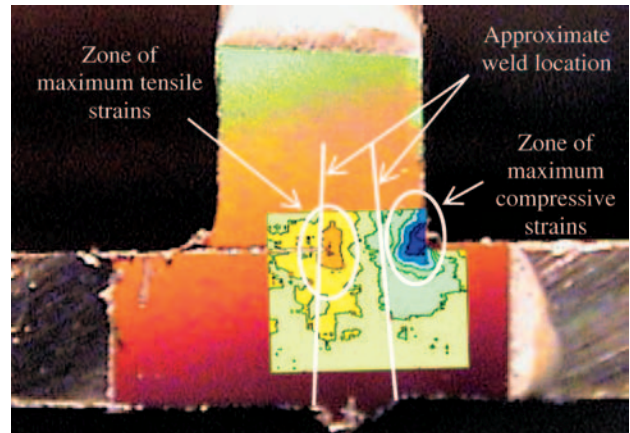


Fig. 8. Strain distributions in B\_3 specimen shown on welded joint background .

Total influence of web bending and web-plate contact on strain distribution in the smallest cross-section of the weld is shown in Fig.9.

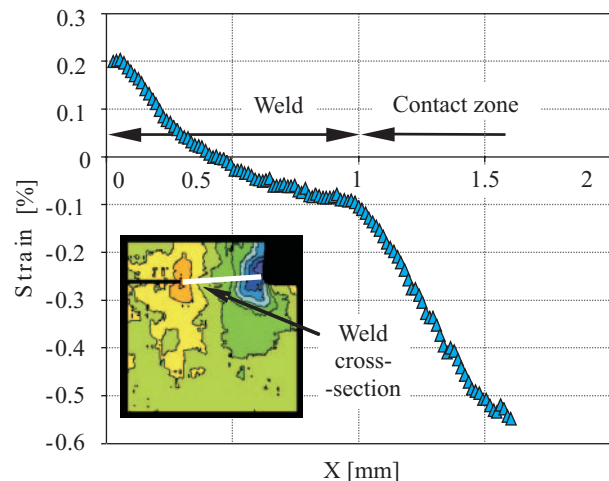


Fig. 9. ( $\epsilon_u$ ) strain distributions in B\_3 specimen, in **u**- direction, along the smallest weld cross-section .

- The largest values of tensile strains ((in **u**- direction) in the analyzed area occurred at the weld edge, and those compressive - in the contact area of web and plate (Fig.9).
- Along with load increasing also strain values in the compressed and tensioned areas were increasing, as well as gradual extending the areas into the plate material was observed.
- The strains in **v**- direction show a symmetrical form respective to the line crossing the smallest cross-section of the weld. (Fig.10).

Detail analysis of their typical distribution shown in Fig.10a, makes it possible to expect a probable character of strain process in the laser weld joint zone, as shown in Fig.10b. The web when displacing against the plate, makes the laser weld built of the welding hardened material, rotating. During the rotating, the weld causes the plate bending and forming two respective zones of tensile and compressive strains in the plate and web material on both sides of the weld.

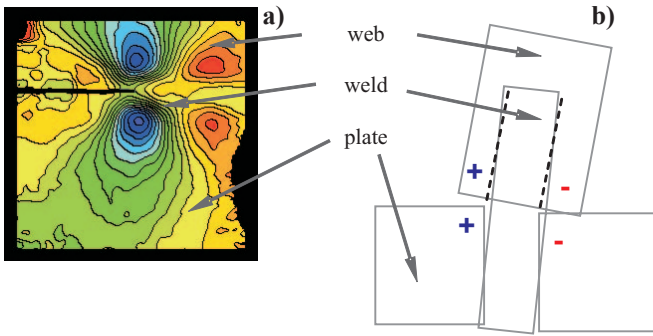


Fig. 10. Schematic diagram of joint deformation -  $(\epsilon_v)$  strains, in v-direction.

### TESTS OF B\_1 ELEMENTARY STRUCTURE UNDER VARIABLE LOADING

During the tests, B\_1 elementary structure was subjected to sinusoidally variable load of the stress ratio  $R = 0$  and the maximum force value  $P_{max} = 25$  kN. For five phases of the loading cycle : A, B, C, D and E images of interference lines in two analyzed directions,  $v$  and  $u$ , were recorded (Fig.11).

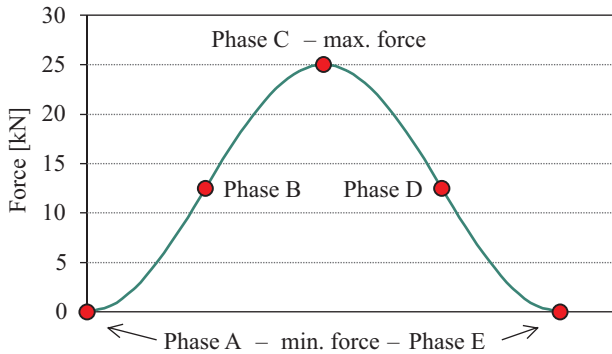


Fig. 11. Strain measurement phases during sinusoidally variable loading.

The strain measurement place is shown in Fig.3. The measurements were executed for every assumed number of load cycles. During the tests, over 20 000 images of interference lines were in total recorded. In Fig.12 the example images of interference lines in the final crack-development phase, are presented.

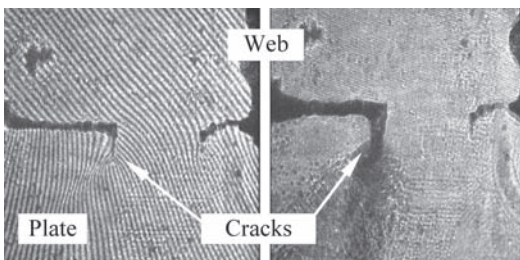


Fig. 12. Image of interference lines in final phase of fatigue life.

In Fig.13 and 14 are shown the example maps of strain distributions in  $v$  and  $u$  directions, respectively, at the maximum values the force  $P$  in load cycle, for some selected load cycles.

In Fig.15 the course of changes of the strains in  $v$ -direction in the joint cross-section Y-Y, is shown. In the diagram an approximate course of the weld connecting the web and plate is marked.

Similarly as in the case of static load the simultaneous presence of geometrical and structural notch generated large strain concentration in the joint zone. During fatigue loading, changes of local strain values additionally occur, and they have different

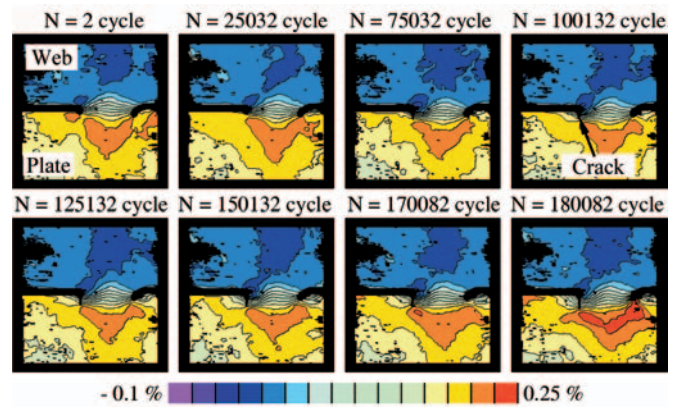


Fig. 13. Strain distributions in v- direction.

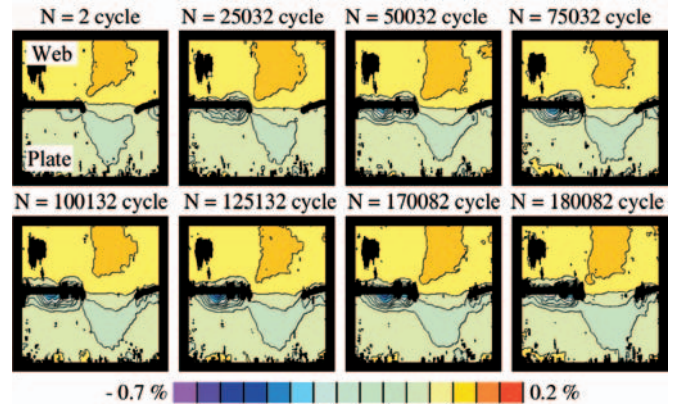


Fig. 14. Strain distributions in u- direction.

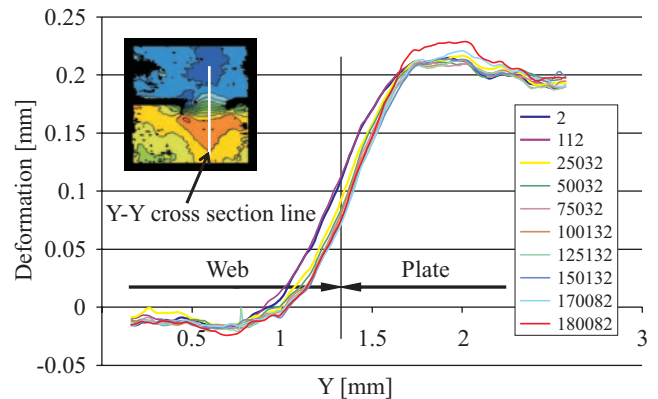


Fig. 15. Strain distribution in v- direction in Y-Y cross-section, recorded in successive load cycles.

character in different joint areas. In the diagram shown in Fig.16 is presented the course of changes of the resultant strains  $\epsilon_{uv}$

(i.e.  $\epsilon_{uv} = \sqrt{\epsilon_u^2 + \epsilon_v^2}$ ) in the point of their maximum values

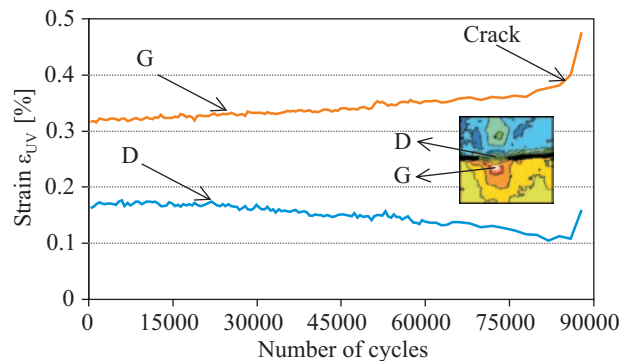


Fig. 16. Run of changes of the maximum value of  $\epsilon_{uv}$  strain during fatigue test.



(marked „G” in Fig.16), and in the transition zone between the plate and web (D). Strain differences in the zones make the strain concentrations in the joint, largest. Along with successive load cycles, values of the maximum strains (G) were increasing and those of the strains (D) – decreasing. It caused the strain gradient increasing during the fatigue test.

To illustrate the strain concentration effect in weld zone, were elaborated the maps of distributions of gradients of  $\epsilon_{uv}$  resultant strain, calculated as :

$$G = \left| \frac{\Delta \epsilon}{\Delta L} \right|$$

where :

$\Delta \epsilon$  – range of % strain change over  $\Delta L$  section

$\Delta L$  – assumed length of the section, corresponding with total distance of six neighbouring measurement points, equal to 0.06 mm.

In Fig.17 is shown the distribution of gradients along the transverse direction respective to load direction, so determined in selected successive load cycles. Their analysis makes it possible to observe that the largest gradient values occur in the transition zone between plate and web, and that along with successive strain cycles the gradient value increases and it a little shifts toward the plate simultaneously.

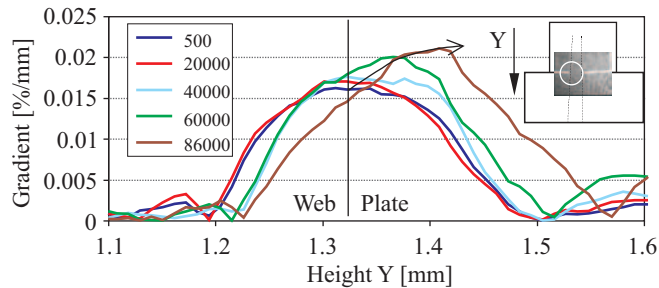


Fig. 17. Gradients of  $\epsilon_{uv}$  strain .

The place of occurrence of the largest strain gradient complies with that of fatigue crack initiation, which can be observed by comparing Fig. 16 and 17.

### TESTS OF B\_3 ELEMENTARY STRUCTURE UNDER VARIABLE LOADING

The B\_3 elementary structure was subjected, similarly as in the case of the B\_1 structure test, to sinusoidally variable load of the stress ratio  $R = 0$  and the maximum force value  $P_{max} = 1.5$  kN. The measurements were performed at five phases (A, B, C, D and E – Fig.11) of selected load cycles.

The strain measurement place is shown in Fig.3. The measurements were performed for every assumed number of load cycles. During the test over 1700 images of interference lines were recorded in total. In Fig.18 are shown the example maps of interference lines, recorded during successive phases of 40 101st load cycle.

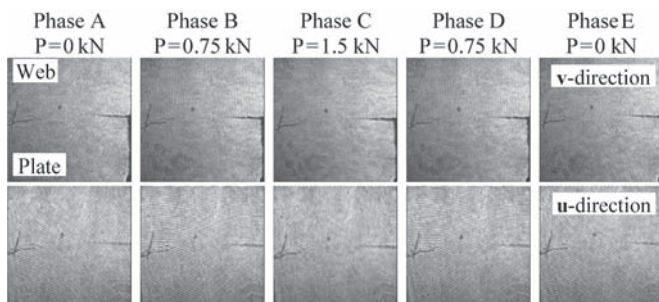


Fig. 18. Example maps of interference lines recorded for the cycle  $N = 40101$  in successive load phases .

Analysis of the recorded interferograms made it possible to determine the strain distributions in the analyzed area. The maps of interference lines, determined during the test, were analyzed with the use of several numerical procedures making it possible to identify particular interference lines and their phases in the analyzed area.

In Fig. 19 and 20 are shown the example maps of interference lines in  $u$  and  $v$  direction, respectively, for the maximum value of the force  $P$ , and selected load cycles.

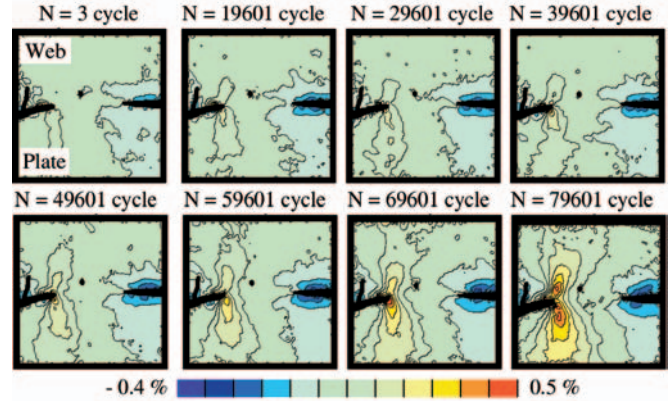
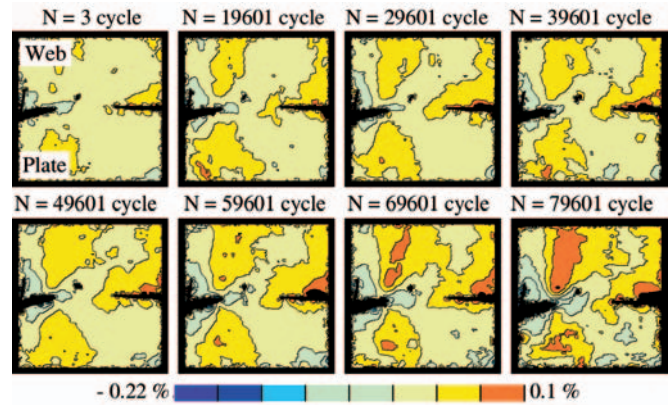


Fig. 19. Strain distributions in  $v$ - direction .



Rys. 20. Strain distributions in  $u$ - direction .

In Fig.21 is presented the course of changes of the strains in  $u$ -direction in the vicinity of the smallest cross-section of the weld and in the contact zone of the plate and web, for selected load cycles. In the diagram an approximate course of the weld connecting the plate and web, is marked.

In the weld zone, like in the case of static load, occurred the strain gradient characteristic for bending, which was additionally amplified by the geometrical notch effect formed by the plate-weld-web transition zone.

Moreover, on the elaborated strain maps compressive strain zones were revealed in the plate-web contact zones.

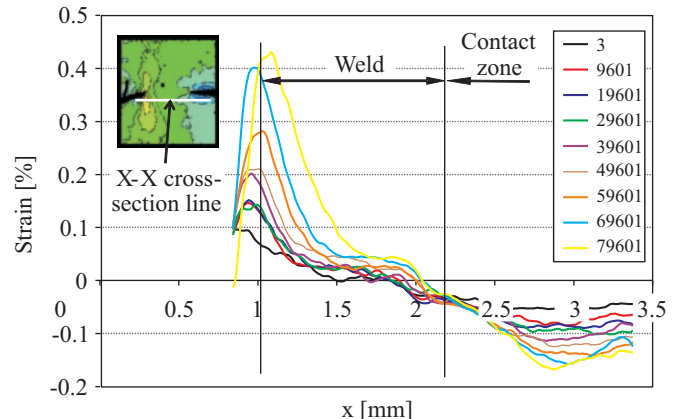


Fig. 21. Strain distribution in  $u$ - direction in X-X cross-section, recorded in successive load cycles .



In the analyzed area the largest values of tensile strains (in **u**-direction) occurred at the weld edge, and those of compressive strains – in the web-plate contact zone.

The strain distributions were changing during successive load cycles, showing an increase of the maximum values of local strains and also an increase of strain gradients in the area of weld edge.

### SUMMARY

- The applied test method based on the LES automatic laser grating extensometer system, made it possible to determine strain distributions in analyzed zones of welded joint of steel sandwich panel structure at various levels of static loading as well as in successive phases of selected cycles of variable loading.
- It made it possible to analyze course of variability of the selected parameters describing strain state in the joint and to indicate their connection with the places of fatigue crack initiation.
- The performed tests yielded the data useful in elaborating the methods for the calculating of fatigue life of structures of the considered kind, with the use of the local approach based on analysing local strains and stresses.
- The presented results may be helpful in further developing sandwich structures themselves and laser welding technique, as well as their design methods as far as avoiding fatigue cracks is concerned.

- Moreover, the results of the performed tests constitute a source base for analyzing the fatigue phenomena and processes which occur in steel sandwich panel structures under cyclic loading.

### BIBLIOGRAPHY

1. Radaj D.: *Review of fatigue strength assessment of non-welded and welded structures based on local parameters*. International Journal of Fatigue No.18/1996
2. Rosochowicz K.: *Problems of the fatigue cracking of ship hulls* (in Polish). Shipbuilding & Shipping Publishing House (Okretnownictwo i Żegluga). Gdańsk, 2000
2. Morrow J.D.: *Fatigue Properties of Metals, Manual*. Society of Automotive Engineers, ISTC Div.4, 1964
3. Boroński D., Szala J.: *Research on zones of fatigue crack initiation and propagation, by using LES laser grating extensometer* (in Polish). Przegląd Mechaniczny No.7-8/2002
5. Boroński D., Szala J.: *Laser grating extensometer LES for fatigue full-field strain analysis*. ECF 14 Fracture Mechanics Beyond 2000, EMAS, 2002
6. Boroński D.: *Cyclic material properties distribution in laser-welded joints*. International Journal of Fatigue, Vol 28/4, 2006
7. Boroński D.: *Experimental analysis of strain distributions in fatigue crack zones* (in Polish). ATR University Reports (Wydawnictwa Uczelniane ATR). Bydgoszcz, 2005
8. Boroński D., Szala J.: *Fatigue tests of laser-welded specimens of sandwich structure models* (in Polish). BZ 8-2003 Report, ATR (University of Technology and Agriculture). Bydgoszcz, 2004

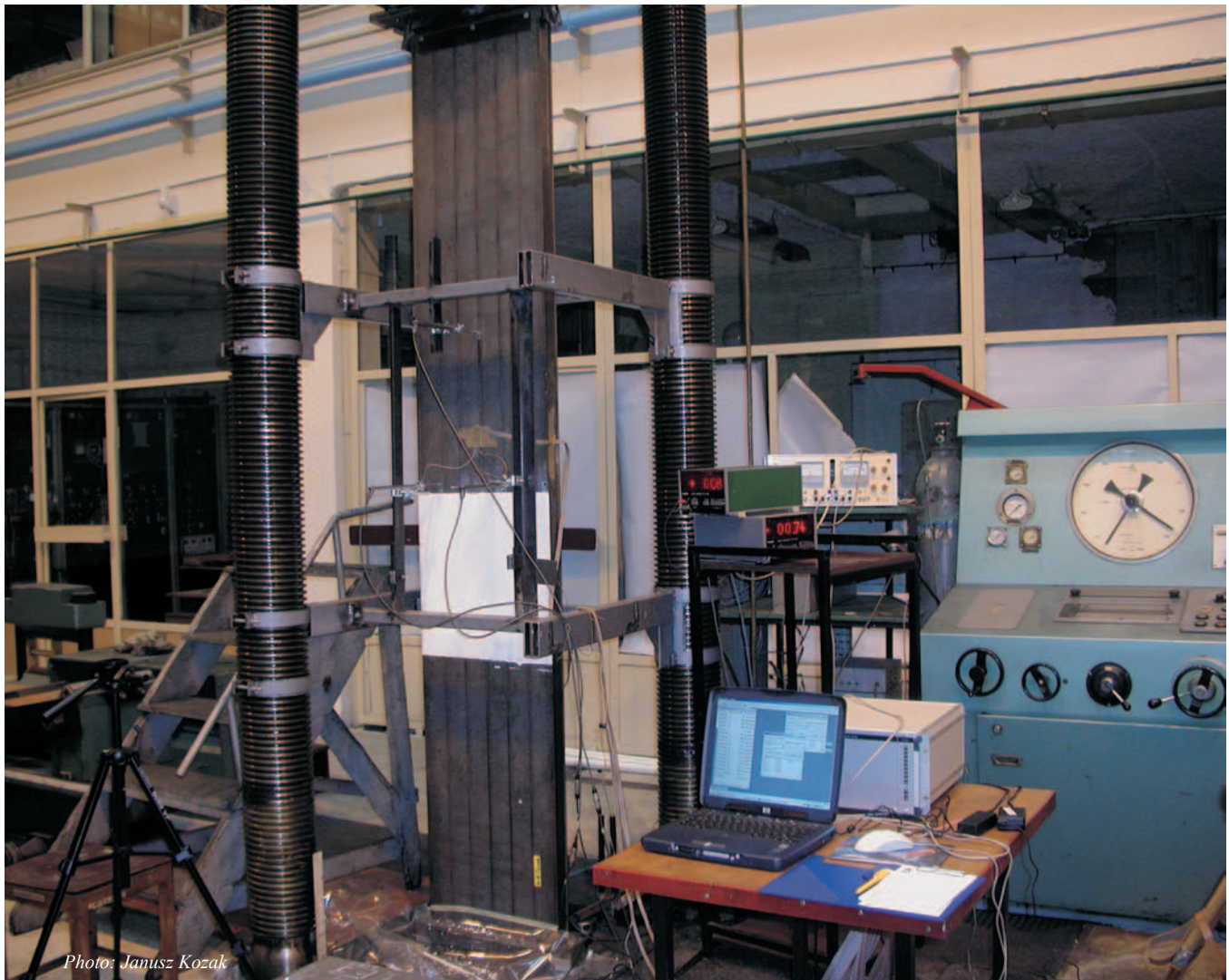


Photo: Janusz Kozak

Sandwich panel model at buckling test stand.